Author Summary

Plasmodium falciparum is responsible for the most severe forms of human malaria. Invasion of host erythrocytes is an essential step of the complex life cycle of this parasite. There is redundancy in many of the interactions involved in this process, such that the parasite can use different sets of receptor–ligand interactions to invade. Here, we demonstrate that the parasite can turn off the expression of some of the proteins that mediate invasion of erythrocytes. Expression can be turned off without alterations in the genetic information of the parasite by using a mechanism known as epigenetic silencing. This is far more flexible than genetic changes, and permits fast, reversible adaptation. Turning on or off the expression of these proteins did not affect the capacity of the parasite to invade normal or modified red cells, which suggests that the variant expression of these genes may be used by the parasite to escape immune responses from the host. Parasite proteins that participate in erythrocyte invasion are important vaccine candidates. Determining which proteins can be turned off is important because vaccines based on single antigens of the parasite that can be turned off without affecting its growth would have little chance of inducing protective immunity.

lines both derived from the cloned parasite line 3D7 but maintained independently for several years, 3D7-A and 3D7-B. These two parasite lines differ dramatically in their capacity to use invasion pathways that permit entry into mutant and enzyme-treated erythrocytes. Remarkably, 3D7-A can invade erythrocytes sequentially treated with neuraminidase plus trypsin, which are completely resistant to invasion by 3D7-B and by all other parasite lines tested [9]. We hypothesised that the different invasion phenotypes of 3D7-A and 3D7-B parasite lines might be accounted for by differences in the expression of some invasion-related genes. In order to identify invasion-related genes under variant expression and to identify the genes responsible for the different invasion phenotypes of 3D7-A and 3D7-B, we performed a microarray comparison of the two parasite lines. While we did not identify the genes responsible for the different invasion phenotypes of the two parasite lines, our experiments led to the identification of invasion-related genes that exhibit variant expression. We also analysed the transcription of invasion-related genes in subclones of 3D7-A and demonstrated the epigenetic nature of the silencing observed for several genes.

Results

Microarray Experiments and Comparison of EBA-140 in 3D7-A and 3D7-B

Microarray experiments were used to compare tightly synchronised schizonts of the parasite lines 3D7-A and 3D7-B (Dataset S1). After excluding from the analysis all genes from the large *var, rif,* and *stevor* families, which are unlikely to participate in the process of erythrocyte invasion, three genes were found to be expressed at very different levels (more than 5-fold difference) between 3D7-A and 3D7-B: *eba-140* (MAL13P1.60, also known as *baebl*), *pfg27/25* (PF13_0011), and *acylCoA binding protein* gene *(acbp)* on Chromosome 14 (*acbp-14,* PF14_0749). The three genes were expressed at much higher levels in 3D7-B than in 3D7-A, with fold differences of 12.4, 11.2, and 7.7, respectively. Most genes presumed to be involved in erythrocyte invasion were expressed at similar levels between 3D7-A and 3D7-B, with the exception of the aforementioned *eba-140* (see Figure 1 for the best-characterised genes). The 95% identical genes *clag3.1* and *clag3.2* were expressed at different levels in the two parasite lines, but the difference was only about 2-fold. However, the high level of identity between the two genes most likely resulted in cross-hybridization of some of the probes and consequent underestimation of the differences (see below).

eba-140 is the only gene among those expressed at very different levels between the two parasite lines that is known to participate in erythrocyte invasion [10], whereas *pfg27/25* is known to have an important role in gametocyte development [11], and the function of *acbp-14* is not known. We first aimed to determine whether lower *eba-140* transcript abundance in 3D7-A compared to that of 3D7-B resulted in lower abundance of EBA-140 protein. Western blot and immunoprecipitation experiments revealed that EBA-140 was abundant both in schizont extracts and in culture supernatants of 3D7-B, but only present at very low levels in 3D7-A (Figure 2A and 2B). The multiple EBA-140-specific bands in Figure 2A and 2B correspond to proteolytic processing products. Furthermore, erythrocyte binding assays revealed a very different composition of proteins that bind to erythrocytes in supernatants from 3D7-A or 3D7-B (Figure 2C). A band of approximately 175 kDa with an identical mobility to EBA-175 (as determined by western blot on samples run side by side, unpublished data) and a band of approximately 152 kDa were observed for both 3D7-A and 3D7-B, but two strong bands with a mobility identical to two of the EBA-140-immunoprecipitated bands were observed only in 3D7-B.

EBA-140 was present by immunofluorescence assay (IFA) in the apical tip of 100% of EBA-175-positive segmented schizonts and free merozoites in 3D7-B, where the two proteins co-localised. The pattern was consistent with the previously described micronemal location for both proteins [10]. In contrast, only a very low percentage (about 7%) of EBA-175 positive schizonts were positive for EBA-140 in 3D7-A (Figure 2D).

Comparison of Radiolabelled Supernatants from 3D7-A and 3D7-B

To detect differences in the expression of invasion-related proteins that might have escaped microarray analysis, we compared radiolabelled culture supernatants from 3D7-A and 3D7-B by SDS-PAGE. Two abundant bands were present in 3D7-A but not in 3D7-B (Figure 3A). A very high molecular mass band corresponds to a form of PfRh2b with an insertion that is present only in 3D7-A [12], as demonstrated by western blot with anti-PfRh2b antibodies on samples run side by side (Figure 3B). The other band has an electrophoretic mobility of approximately 148 kDa and forms a doublet with a band of slightly higher mobility. Because the size of these bands is similar to the size of RhopH1/Clag, we immunoprecipitated supernatants of the two lines with an anti-RhopH2 monoclonal antibody that immunoprecipitates the whole RhopH complex. The immunoprecipitated complex contained an additional band in 3D7-A with an identical mobility to the band present in supernatants of 3D7-A but not of 3D7-B, indicating that the protein present only in 3D7-A supernatants is part of the RhopH complex (Figure 3C). Mass

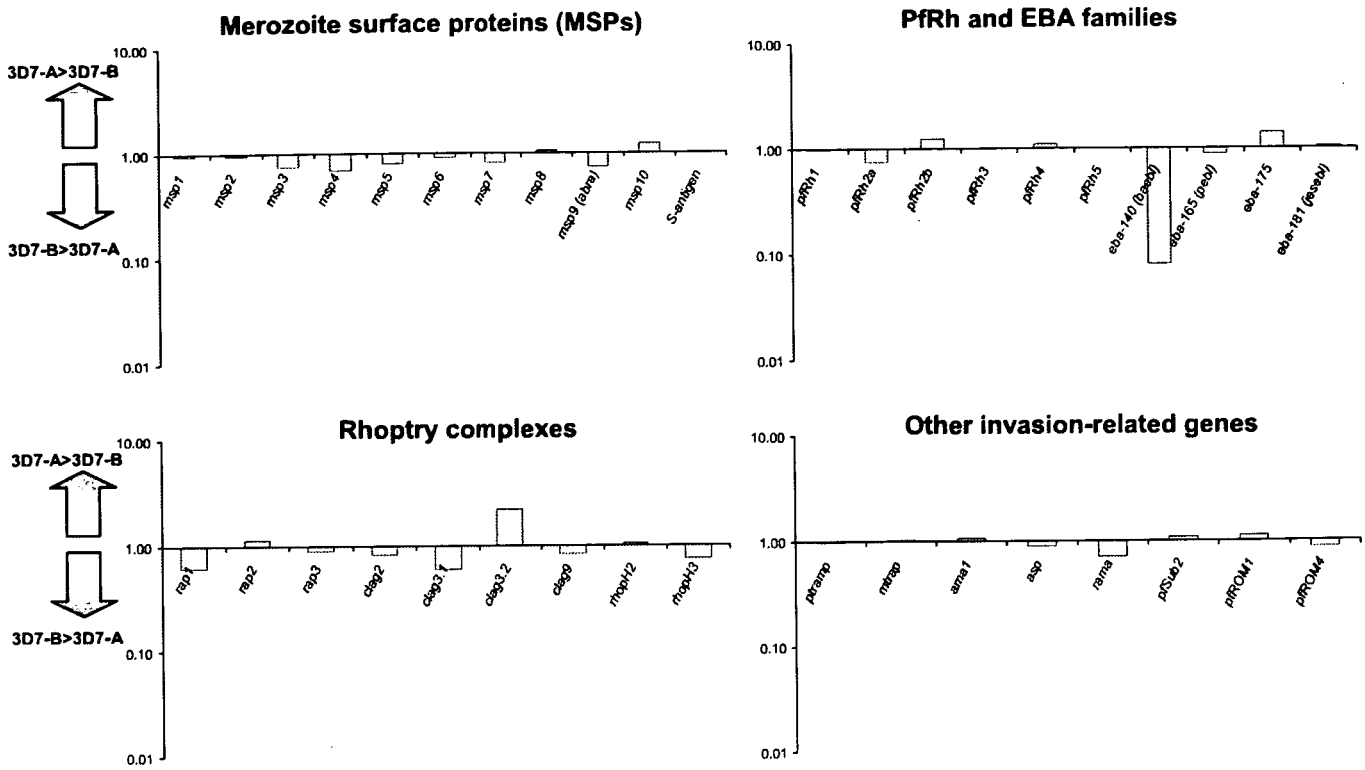

Figure 1. Microarray Comparison of Expression of Invasion-Related Genes between 3D7-A and 3D7-B Schizonts

Values correspond to the ratio of expression in 3D7-A versus 3D7-B. Values for each parasite line are the average of two experiments.

doi:10.1371/journal.ppat.0030107.g001

spectrometry analysis revealed the identity of this polypeptide as Clag3.2 (PFC0110w) (25% coverage), whereas the lower band of the doublet (also present in 3D7-B, arrowhead in Figure 3A) was identified as Clag3.1 (PFC0120w) in both parasite lines (33% coverage). Despite the 95% identity between the two proteins, the identification was unambiguous because it was based on three peptides that were specific for one or the other protein (Table 1). As expected from these results, reverse transcriptase (RT)-PCR analysis revealed that *clag3.1* transcripts are present at similar levels in 3D7-A and 3D7-B schizonts, but *clag3.2* transcripts are almost absent in 3D7-B (Figure 3D).

Expression of Invasion Ligands in Subclones of 3D7-A

To determine whether further heterogeneity in the expression of invasion-related genes occurs in the cloned parasite line 3D7, we analysed expression of these genes in 11 subclones of 3D7-A (described in Materials and Methods). Silver-stained SDS-PAGE analysis of culture supernatants from these 11 subclones revealed that all of them expressed either Clag3.1 or Clag3.2, but none of them expressed both (Figure 4A, top panels). Each subclone had gone through at least 11 cycles of replication from a single parasite to harvesting for analysis. The subclones reflect the clonally transmitted expression pattern of the individual parasites from which they originated. This result indicates that 3D7-A is a mixture of parasites expressing one or the other protein. Mutually exclusive expression of the two genes was confirmed by semi-quantitative RT-PCR (Figure 4A, middle panels). All clones that expressed *clag3.1* at high levels had only low-level expression of *clag3.2* and vice versa. Furthermore, another member of the *clag* family, *clag2*, also showed clonal variant expression between the subclones, whereas *clag8* and *clag9* were expressed at very similar levels in all subclones (Figure 4A). Western blot analysis with antibodies specific for Clag2 and Clag3.2 confirmed that low levels of transcripts resulted in low abundance or absence of the corresponding proteins in culture supernatants (Figure 4A, bottom panels). Expression patterns remained stable over continuous culture for at least one additional month (Figure S1A). Interestingly, a stock of the cloned line HB3 at Ehime University (Japan) derived from HB3B, which had been passed through chimpanzees [13], expressed only *clag3.1*, but a stock at the same university derived from HB3A (prior to chimpanzee passage) expressed only *clag3.2*, supporting the idea of mutually exclusive expression and switching between the two genes (Figure S2). HB3 at the National Institute for Medical Research (United Kingdom) and W2mef lines only expressed *clag3.1* at detectable levels (unpublished data).

We also analysed by RT-PCR the expression of members of other multigene families involved in erythrocyte invasion. All members of the *eba* family were expressed at similar levels in the 11 3D7-A subclones except for *eba-140*, which was silenced in most subclones but expressed at levels similar to that of 3D7-B in two of them (Figure 4B). Western blot analysis of schizont extracts revealed that abundance of EBA-140 protein correlated well with transcript abundance (Figure 4B, bottom panels). The pattern of expression of EBA-140 in 3D7-A subclones was fully consistent with the result of IFA experiments (Figure 2D).

Expression of some members of the PfRh family had previously been described as varying between non-isogenic

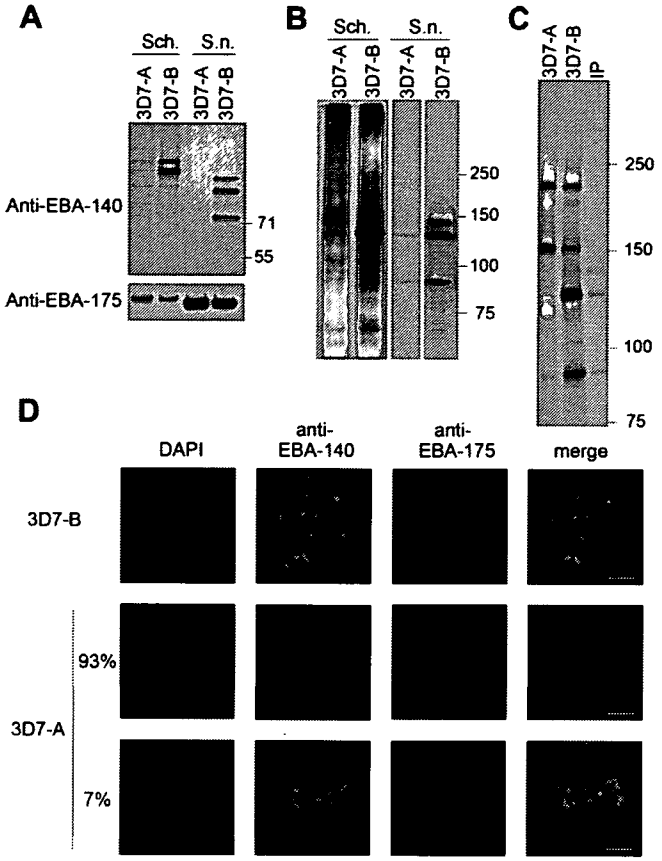

Figure 2. Analysis of EBA-140 in 3D7-A and 3D7-B

(A) Western blot analysis of schizonts extracts (Sch.) or culture supernatants (S.n.) probed with rat anti-EBA-140 antibodies. The same membrane was re-probed with rabbit anti-EBA-175 antibodies to control for the amount of stage-specific material. The position of SeeBlue Plus2 pre-stained standards (Invitrogen) is shown (kDa).

(B) Immunoprecipitation of NP-40-extracted schizonts and culture supernatants with anti-EBA-140 antibodies. The position of Precision Plus All Blue pre-stained standards (Bio-Rad, http://www.bio-rad.com/) is shown.

(C) Erythrocyte binding assay with radiolabelled supernatants from 3D7-A and 3D7-B. The lane IP corresponds to 3D7-B supernatant immunoprecipitated with anti-EBA-140 antibodies.

(D) IFA of 3D7-A and 3D7-B schizonts with rabbit anti-EBA-140 and mouse anti-EBA-175 antibodies. Middle and lower panels are representative of 93% and 7% of EBA-175-positive 3D7-A schizonts, respectively. Scale bar = 5 μm.

doi:10.1371/journal.ppat.0030107.g002

parasite lines [14–16]. We found only small differences in the level of expression of these genes among our subclones, with the exception of *pfRh2b* that was expressed at low levels in the subclones 4D and W4-1 to W4-4 (Figures 4C and S1B). See Text S1 for an explanation of the confounding effect of small differences in the stage of the parasites and the controls developed to overcome this difficulty.

Variant expression among subclones was also observed for two genes, *pfg27/25* and *acbp-14*, which were expressed at higher levels in 3D7-B than in 3D7-A according to the microarray analysis (Figure 4D). Analysis of the subclones revealed that these genes are also silenced in some individual parasites but expressed at levels similar to that of 3D7-B in others. *acbp-14* belongs to a four-gene family [17], but expression of the other genes of this family was similar in all 3D7-A subclones (Figure 4D and Text S1).

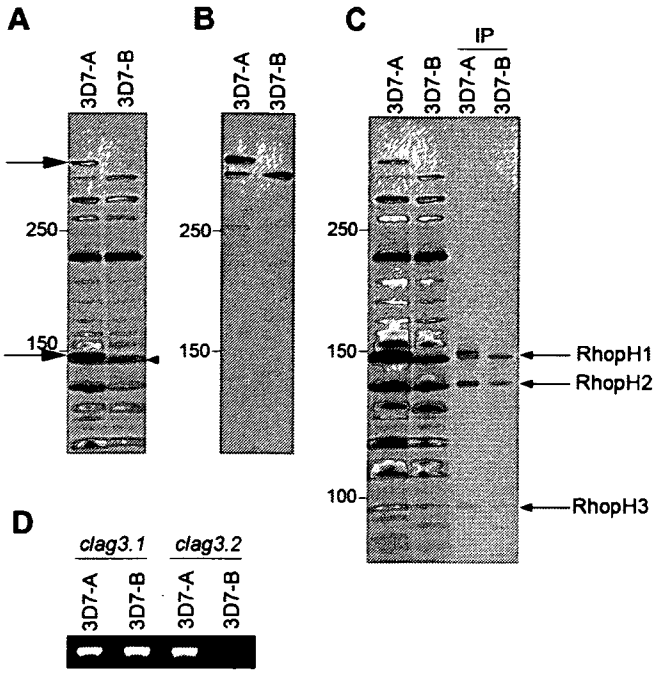

Figure 3. Comparison of Proteins Secreted to the Culture Supernatant between 3D7-A and 3D7-B

(A) Radiolabelled culture supernatants run on 20-cm-long 6% SDS-PAGE. The arrows indicate bands present in supernatants from 3D7-A but not from 3D7-B. The arrowhead indicates the band that forms a doublet with the 148-kDa band present only in 3D7-A.

(B) Western blot of two lanes identical to those in (A) and run contiguously, probed with rabbit anti-PfRh2b antibodies.

(C) Culture supernatants run side by side with identical supernatants immunoprecipitated with the monoclonal antibody 61.3 against RhopH2 (lanes IP). The position of the three members of the RhopH complex is indicated.

(D) RT-PCR analysis of *clag3.1* and *clag3.2* in RNAs from 3D7-A and 3D7-B schizonts.

doi:10.1371/journal.ppat.0030107.g003

Invasion Phenotype of 3D7-A-Derived Parasite Lines That Differ in the Expression of Invasion Ligands

Despite differences in the expression of several invasion-related proteins, all the 3D7-A subclones tested had very similar growth rates as determined in a one-cycle FACS-based growth assay (Table 2). Likewise, the capacity to invade erythrocytes treated with various enzymes was very similar among all the 3D7-A subclones tested and indistinguishable from that of the parental 3D7-A, but different from that of 3D7-B (see Figure 5A and Figure 5F for comparison). All the 3D7-A subclones invaded erythrocytes sequentially treated with neuraminidase plus trypsin, which are completely resistant to invasion by 3D7-B. Thus, the expression status of *clag2, clag3.1, clag3.2, eba-140, acbp-14, pfg27/25,* or *pfRh2b* did not affect the invasion pathways used by the parasites. This was confirmed by selection-based experiments (Figure S3).

We used an additional approach to confirm that silencing of *eba-140* does not alter the invasion phenotype of the parasites and is not necessary for the invasion of neuraminidase plus trypsin–treated erythrocytes. We expressed *eba-140* in 3D7-A parasites under the control of its own promoter on an episome. We tried three different constructs that contained 0, 797, or 1,331 bp of the region upstream from the *eba-140* start codon to drive the expression of the episomal

Table 1. Mass Spectrometry Identification of Clag3.1 and Clag3.2

Peptide Sequence[a]	Protein	Expected *m/z*	Observed *m/z*[b]	
			Top	Bottom
(K) EAQEESSPIGDHGTFFRK	Clag3.1	2034.952	–	2034.959
(K) ESSPIGDHGTFFRK	Clag3.2	1577.771	1577.773	–
(K) TLYVHLLNLTGLLNYDTR	Clag3.1	2119.155	–	2119.157
(K) TLYVHLLNLTGLLNHDTR	Clag3.2	2093.151	2093.170	–
(K) FKEWMNSSPAGFYFSNYQNPYIR	Clag3.1	2894.288	–	2894.213
(K) FKEWMDSSPAGFYFSNYQNPYIR	Clag3.2	2847.288	2847.240	–

[a]Each pair of sequences corresponds to equivalent positions in an alignment of Clag3.1 and Clag3.2.
[b]Refers to the *m/z* value that matches the peptide, in the top or the bottom band of the doublet under analysis (see text). The – sign indicates that no matching peptide was found in a band.
doi:10.1371/journal.ppat.0030107.t001

transgene (Figure 5B). Transfection with these constructs resulted in production of EBA-140 protein only when the longer version of the 5′ region was used (E140-1300), as determined by western blot (Figure 5C). The timing of expression of the episomal *eba-140* was correct, because transcripts of this transgene were undetectable by RT-PCR in ring or trophozoite stages, but were highly abundant in schizonts, as observed for authentic *eba-140* in 3D7-B (Figure 5D). Furthermore, episomally expressed EBA-140 co-localised with EBA-175 by IFA (Figure 5E), indicating that it is correctly located in the apical organelles. Altogether, these results indicate that this large protein can be correctly expressed from an episome. However, only 65% of EBA-175-positive schizonts were EBA-140 positive, probably due to defective segregation of the episome.

E140-1300-transfected 3D7-A parasites had an invasion phenotype indistinguishable from that of 3D7-A, but clearly distinct from that of 3D7-B (Figure 5F). Despite expressing EBA-140, these parasites invaded erythrocytes double-treated with neuraminidase plus trypsin as efficiently as 3D7-A parasites, in contrast to 3D7-B parasites that completely failed to invade them. Invasion assays were performed in the absence of drug. To rule out the possibility that only parasites that had lost the episome (and consequently were not expressing EBA-140) were able to invade double-treated erythrocytes, parasites that had invaded these erythrocytes were placed back under drug pressure and found to have survival rates similar to those invading control erythrocytes.

Chromosomal Structure of *eba-140, clag3.1,* and *clag3.2* Loci in Parasite Lines That Vary in the Expression of These Genes

To determine whether there were genetic differences in the *eba-140, clag3.1,* or *clag3.2* genes associated with their expression status, we analysed these loci in parasite lines where the genes were either expressed or not. Southern blot analysis of the *eba-140* locus, covering the open reading frame (ORF), and also 4.1 kb upstream from the start codon and 3.8 kb downstream from the stop codon, did not reveal any difference between 3D7-A and 3D7-B parasites (Figure 6A and 6C). Furthermore, an *eba-140*-specific PCR product was amplified from genomic DNA from all 3D7-A subclones, including those that do not express the gene. Similarly, Southern blot analysis of the chromosomal region where *clag3.1* and *clag3.2* are located, including the region between the two genes and 2.9 kb upstream from the start codon of *clag3.2* and 6.4 kb downstream from the *clag3.1* stop codon, did not reveal any difference between parasite lines that only express *clag3.1* at high levels (3D7-B and 4D), a parasite line that only expresses *clag3.2* (10E), and 3D7-A, which is a mixture of parasites that express one or the other gene (Figure 6B and 6D). Altogether, these results rule out the possibility that low expression of *eba-140, clag3.1,* or *clag3.2* was associated with major chromosomal rearrangements, deletions, or recombination of the two *clag* genes in Chromosome 3 to form a single gene.

Furthermore, direct sequencing of PCR products spanning the ORF of *eba-140* and 1.3 kb upstream from its start codon did not reveal any difference between 3D7-A and 3D7-B. We also PCR amplified the full *clag3.1* and *clag3.2* ORFs in these two parasite lines with primers in their divergent 5′ and 3′ UTR sequences. Sequencing of these PCR products revealed no difference between the two parasite lines or compared with the published sequences for the genes, which rules out the possibility that a gene conversion event had occurred.

Transcriptional Analysis of the Left Subtelomeric Region of Chromosome 13

The two genes expressed at most different levels between 3D7-A and 3D7-B as determined by microarray analysis, *eba-140* and *pfg27/25,* are located in the left subtelomeric region of Chromosome 13 (Figure 7A), at a distance of 89.4 and 121.8 kb from the telomere, respectively. This is suggestive of coordinated regional silencing of this subtelomeric zone in 3D7-A. None of the genes located between *eba-140* and *pfg27/25* or between the telomere and *eba-140* is expressed at high levels in schizonts [18,19]; thus, our microarray experiments were unable to determine whether they are also differentially expressed between 3D7-A and 3D7-B. We prepared RNA from tightly synchronised ring- (11–16 h), trophozoite- (23–28 h), or schizont-stage parasites (39 h and 30 min to 44h and 30min for 3D7-A, 41–46 h for 3D7-B) and performed RT-PCR analysis of *eba-140, pfg27/25,* and four additional genes located in this chromosomal region (Figures 5D and 7). Two of the genes with a peak of expression in rings, *gbph2* and MAL13P1.61, were expressed at slightly higher levels in

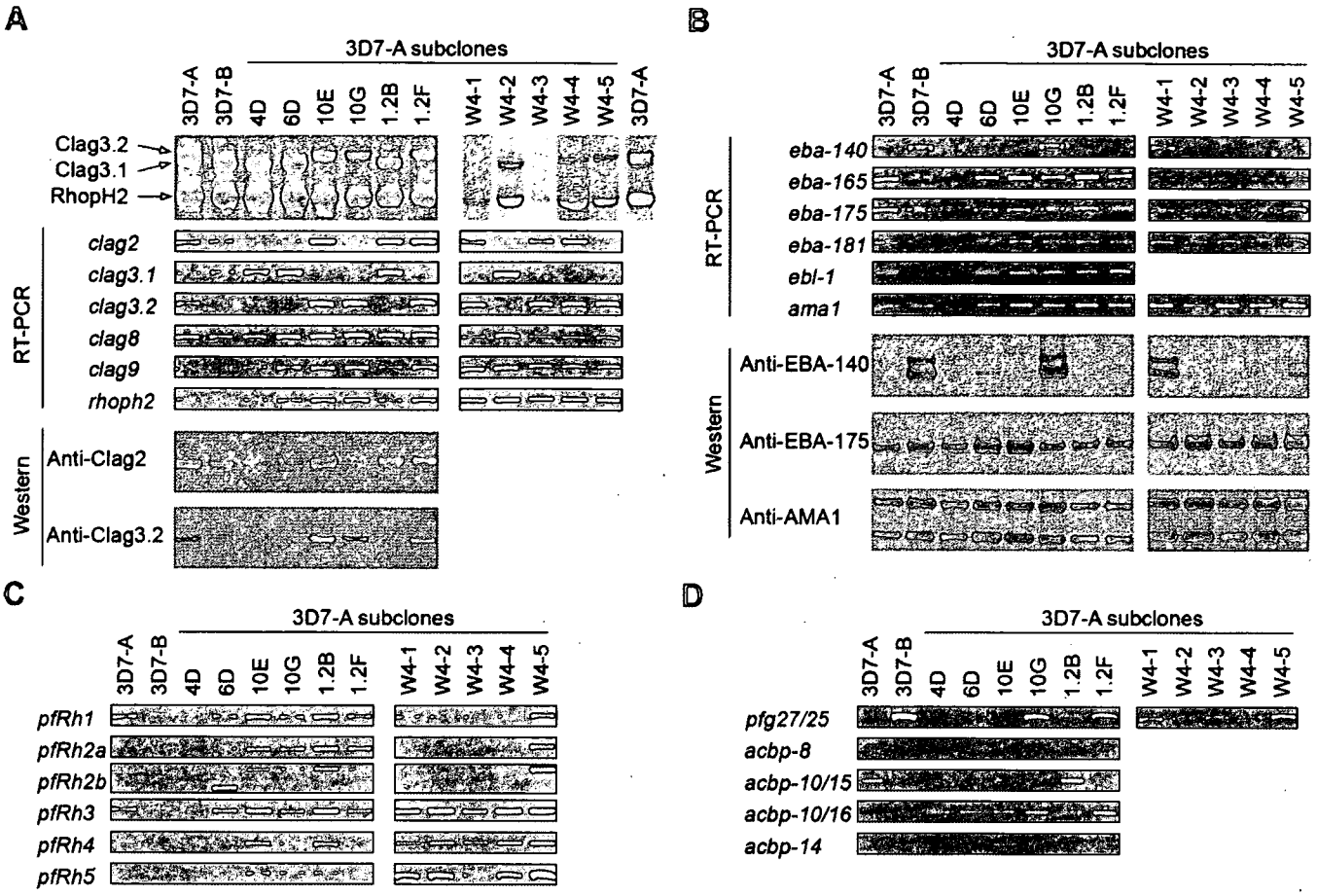

Figure 4. Expression of Invasion-Related Genes in Subclones of 3D7-A

(A) Analysis of expression of the *rhoph1/clag* family. Top, silver staining of RhopH components in concentrated, Albumax-free culture supernatants from 3D7-A, 3D7-B, and 11 subclones of 3D7-A resolved in 20 cm 6% SDS-PAGE. Middle, RT-PCR analysis from RNA of tightly synchronised schizonts. cDNA samples were the same across the four panels. The single copy *rhoph2* gene was used to control the amount of stage-specific cDNA. The intensity of bands in left and right columns cannot be directly compared (in any of the panels) because they correspond to separate experiments. Bottom, same samples as in the top panel analysed by western blot with anti-Clag2 and anti-Clag3.2 antibodies.

(B) Analysis of expression of members of the *eba* family. Top panels, RT-PCR analysis. The single-copy *ama1* gene was used to control the amount of stage-specific cDNA. Lower panels, western blot analysis of schizont extracts with rat anti-EBA-140 antibodies. The same membranes were probed with rabbit anti-EBA-175 and mouse anti-AMA1 antibodies.

(C) RT-PCR analysis of expression of genes of the *pfRh* family. The timing of expression of these genes is similar to that of *ama1;* thus, RT-PCR analysis of this gene in (B) controls the amount of stage-specific cDNA.

(D) RT-PCR analysis of genes expressed at very different levels between 3D7-A and 3D7-B, and of other members of the *acbp* gene family: *acbp* gene in Chromosomes 8 (PF08_0099), 10 (PF10_0015 and PF10_0016), and 14 (PF14_0749). See Text S1 for the control of stage-specific cDNA.

doi:10.1371/journal.ppat.0030107.g004

3D7-B than in 3D7-A, and the same was true for the member of the *rif* family, PF13_0006, which was unexpectedly expressed in schizonts. On the other hand, PF13_0076 was expressed at all stages and at similar levels in both parasite lines (Figure 7B). Thus, higher expression in 3D7-B than in 3D7-A occurred for several genes in this chromosomal region, but different genes were affected to different extents. The most marked differences were observed for genes expressed in late schizonts (*eba-140* and *pfg27/25*).

In Situ Activation of *eba-140* by Insertion of a Drug Resistance Marker Gene in Its Vicinity

Integration of the construct E140–0 (Figure 5B) in the *eba-140* locus by a single-recombination event was achieved by cycling E140–0-transfected 3D7-A parasites for two cycles on/off drug and confirmed by Southern blot (Figure 8A and 8B). The integration of the construct resulted in the duplication of the *eba-140* gene, but only one copy was preceded by sequences with promoter activity (Figures 8A and 5B). Western blot analysis revealed that integration of this plasmid resulted in expression of the *eba-140* gene, though at a lower level than in 3D7-B (Figure 8C).

E140–0-transfected and -drug-cycled 3D7-A parasites were subcloned by limiting dilution. Five of the resulting subclones were analysed by Southern blot, which revealed that three of them had integrated one copy of the gene (W4–1, W4–2, and W4–5), whereas one had integrated two or more copies (W4–3) and one was wild type (W4–4) (Figure 8B). Subcloning was performed in the absence of drug pressure. RT-PCR and western blot analysis of these subclones revealed that only one of them (W4–1) expressed EBA-140 at high levels, whereas all the other subclones expressed it at low levels similar to that of the parental 3D7-A (Figure 4B). The three subclones that had one copy of the construct integrated were

Table 2. Growth Rate of 3D7-A Subclones

Subclone	Growth Rate[a]
6D	9.7 (0.8)
10E	10.6 (0.2)
10G	10.1 (0.3)
1.2B	11.2 (0.9)
W4-1	9.9 (0.2)
W4-5	10.4 (0.2)

[a]Figures are the average of two independent experiments. Standard deviation is shown in brackets.

doi:10.1371/journal.ppat.0030107.t002

maintained in parallel either in the absence or presence of drug selection for 1 mo, and RNA from tightly synchronised schizonts of the resulting populations was analysed by RT-PCR. The presence of the drug resulted in a large (W4-1 and W4-2) or moderate (W4-5) increase in the abundance of transcripts of the drug resistance gene *hdhfr*. The increase was paralleled by a dramatic increase in the abundance of *eba-140* transcripts in the clone W4-2, whereas expression of this gene was not affected in the clone W4-1, which already expressed *eba-140* at high levels before drug selection, and only moderately increased in the clone W4-5 (Figure 8D). This result indicates that insertion of a gene *(hdhfr)* that is forced to be active (by drug selection) in the vicinity of *eba-140* can cause the activation of this gene. Thus, *eba-140* can be activated in situ, ruling out the possibility that undetected genetic changes were responsible for the silencing and indicating that silencing was epigenetic. Expression of the gene *pfg27/25,* which is more distal to the telomere than *eba140* and was already active in the absence of drug in the three clones (Figure 4D), was affected to a lower extent (Figure 8D).

Discussion

The process of erythrocyte invasion by merozoites of *P. falciparum* involves several essential, highly conserved interactions as well as dispensable, redundant interactions. Here we show that several of the genes responsible for the latter can be epigenetically silenced. Some members of the *pfRh* family had been shown to vary in expression between non-isogenic cloned parasite lines [14,15] and among field isolates [16]. Furthermore, switching from sialic acid-dependent into sialic acid-independent invasion in the two related parasite lines W2mef and Dd2 involved increased expression of PfRh4 [4,20]. Here, we extend the observation of variant expression to several other invasion-related gene families in isogenic parasite lines and demonstrate that silencing is transmitted epigenetically.

The comparison of the two isogenic parasite lines 3D7-A and 3D7-B revealed differences in the expression of *eba-140, clag3.2, pfg27/25,* and *acbp-14*. To determine whether further heterogeneity exists within the cloned line 3D7, we analysed the expression of invasion-related genes in 11 subclones of 3D7-A, which reflect the pattern of expression in the 11 3D7-A individual parasites from which they originated. Clonal variant expression was detected for three additional genes, *clag2, clag3.1,* and *pfRh2b*. In all cases tested, mRNA abundance reflected protein abundance. Thus, 3D7-A is a mosaic of parasites expressing different combinations of invasion proteins. It will be important to determine to what extent this mosaicism occurs in natural parasite populations.

A main feature of all the invasion-related genes showing variant expression is that they belong to small multigene families. The *var* genes, which are the paradigm of variant expression in *Plasmodium,* are also part of a multigene family, though of a much larger size. *var* genes, which participate in both immune evasion and cytoadhesion of infected erythrocytes, exhibit mutually exclusive expression, such that only one gene of the family is expressed at a time [21]. In the case of invasion-related multigene families, we observed mutually exclusive expression for two members of the *clag* family, *clag3.1* and *clag3.2*.

We did not detect any DNA alteration associated with the active or silent state of invasion-related genes. Although we cannot exclude the possibility of minor alterations that escaped our analysis, or that regulatory regions where alterations occurred were located in distant regions of the chromosome, the most plausible explanation is that, at least in the cases of *clag3.1, clag3.2,* and *eba-140,* silencing was transmitted epigenetically. This is again reminiscent of the situation for *var* genes, which switch from a silent to an active state without detectable DNA alterations [21] and which are epigenetically silenced in a process that involves modifications of the chromatin structure [22,23]. Furthermore, approximately two-thirds of *var* genes and the majority of members of small invasion-related multigene families for which we detected variant expression are located in subtelomeric positions (Figure S4), though *var* genes are always more proximal to the telomere. It will be important to determine whether the subtelomeric location of these invasion-related genes is critical for their variant expression or, instead, is related to their evolution.

In addition to the absence of genetic alterations between an active and a silenced state, reversibility and region-specific rather than sequence-specific effects are hallmarks of epigenetic silencing and heterochromatin. Both were demonstrated for the silencing of *eba-140*. Insertion of the drug resistance gene *hdhfr* in the vicinity of the *eba-140* locus and subsequent drug pressure resulted in the in situ activation of this gene in some subclones. This suggests that activation of *hdhfr* disrupted a compact, "closed" conformation of the chromatin around this locus and forced the transition to a more relaxed, transcriptionally active conformation that spread into the neighbour *eba-140*. Furthermore, silencing of *eba-140* in 3D7-A was somehow coordinated with silencing of another gene located in the same subtelomeric region, *pfg27/25*. This locus was silenced in some subclones of 3D7-A but expressed in others, but in all cases where the more telomere proximal *eba-140* gene was active, *pfg27/25* was also active. This suggests a model in which silenced chromatin would spread from a telomeric position. The extent of the silenced area would vary stochastically between individual parasites, but once established it would be clonally inherited, which would explain the variegated expression of the two genes in the different subclones. In some subclones, the silenced area would spread as far into the chromosome as the *pfg27/25* locus, while in others it would only reach *eba-140* but not *pfg27/25,* and in others it would not even reach *eba-140*. However, the observation that other genes located in the

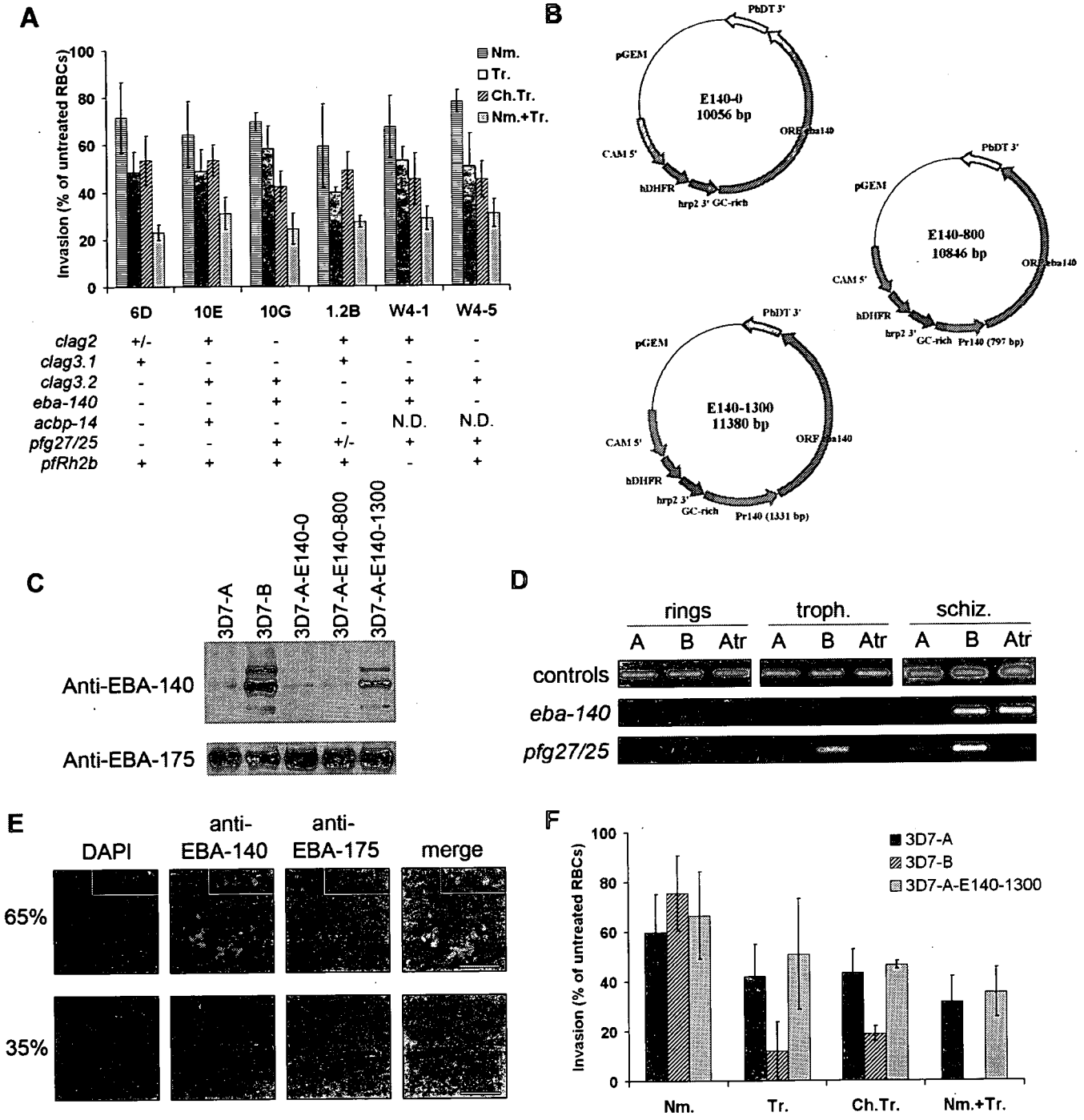

Figure 5. Invasion Phenotypes Associated with the Expression Status of Variantly Expressed Invasion-Related Genes

(A) Invasion phenotype of 3D7-A subclones. Values correspond to percent of invasion into untreated erythrocytes and are the average of three to four independent experiments, with 95% confidence interval. Expression of genes that vary in expression between the subclones is shown underneath. The signs + and − correspond to high or low expression relative to other subclones. N.D., not determined; Nm., neuraminidase; Tr., trypsin; Ch.Tr, chymotrypsin; Nm.+Tr, neuraminidase plus trypsin.

(B) Scheme of the plasmids transfected in 3D7-A parasites for the episomal expression of EBA-140.

(C) Western blot analysis of schizont extracts, as in Figure 2A. Lanes are 3D7-A, 3D7-B, or 3D7-A parasites transfected with the different plasmids, as indicated.

(D) RT-PCR analysis at different stages of the life cycle in 3D7-A (lanes A), 3D7-B (lanes B), and E140-1300-transfected 3D7-A (lanes Atr). The amount of stage-specific cDNA was controlled by amplification of the genes PF13_0275 (rings), PF10_0121 (trophozoites), and *ama1* (PF11_0344) (schizonts).

(E) IFA of E140-1300-transfected 3D7-A schizonts. Top and lower panels are representative of 65% and 35% of EBA-175-positive schizonts, respectively. The inserts in the top panels are free merozoites. Scale bar = 5 μm.

(F) Invasion phenotype of E140-1300-transfected 3D7-A parasites compared to that of 3D7-A and 3D7-B. Values correspond to percent of invasion into untreated erythrocytes and are the average of two independent experiments, with 95% confidence interval.

doi:10.1371/journal.ppat.0030107.g005

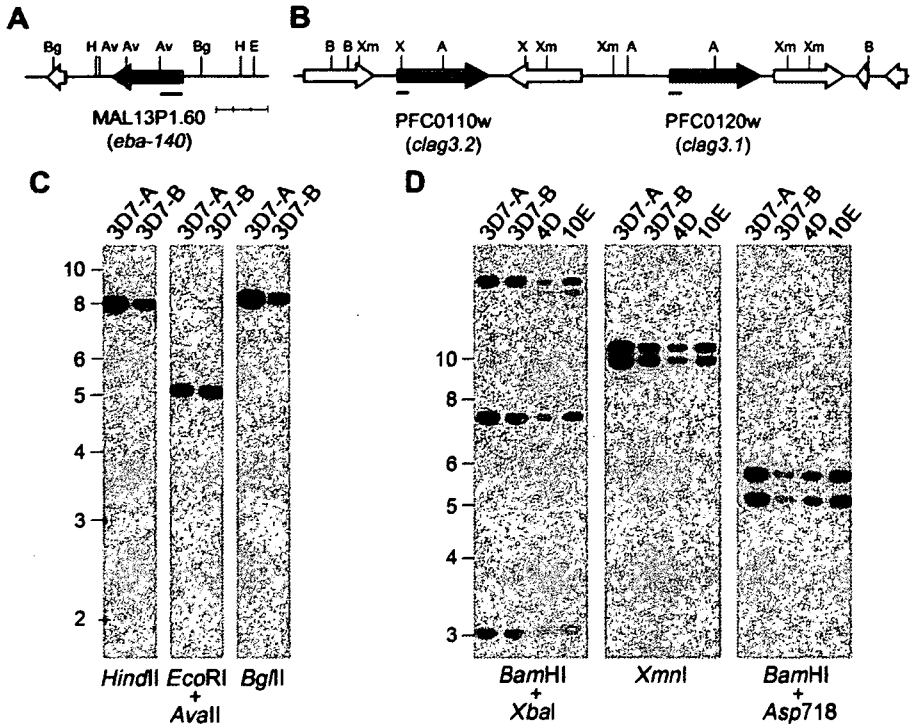

Figure 6. Southern Blot Analysis of *eba-140, clag3.1,* and *clag3.2* Loci

(A and B) Genomic organization around the loci under study, showing the restriction sites used for Southern blot analysis and the genes annotated in PlasmoDB (block arrows, genes under analysis in grey, neighbours in white). Diagrams are to scale. The scale bar corresponds to 3 kb. Restriction sites are BglII (Bg), HindII (H), AvaII (Av), EcoRI (E), BamHI (B), XmnI (Xm), Asp718 (A), and XbaI (X). The short lines underneath the genes indicate the position of the probes used.

(C and D) Southern blot analysis. The probes used were a 1,304-bp BglII-AvaII restriction fragment from the E140–0 plasmid corresponding to the beginning of the *eba-140* ORF (C) or a 1:1 mixture of PCR-amplified fragments of about 700 bp corresponding to the beginning of the ORF of *clag3.1* and *clag3.2* (D). The position of DNA size markers is indicated (kb).

doi:10.1371/journal.ppat.0030107.g006

same region were only silenced to a lower extent or not silenced at all does not support this model, and suggests that either the silenced chromatin structure is only formed late in the life cycle of the parasite, or a mechanism other than heterochromatin spreading is responsible for the coordinated silencing of these genes. Further experiments will be needed to distinguish between these two possibilities. It will also be important to determine whether transcripts from PF13_0076 in schizonts, which occurred at similar levels in 3D7-A and 3D7-B, represent active transcription at this stage or carry over of mRNA transcribed in previous stages.

In contrast to the apparently region-specific, sequence-independent variegated silencing of the *eba-140* locus, silencing of *clag3.1* or *clag3.2* was promoter specific, because the two genes lie adjacent to each other in the genome and expression was mutually exclusive. This situation is more similar to that observed for *var* genes, where one gene can be activated while its neighbours remain silenced [24]. The chromosomal organization of *clag3.1* and *clag3.2* resembles that of two other invasion-related genes with a high level of identity, *pfRh2a* and *pfRh2b,* which lie adjacent to each other near the centromeric region of Chromosome 13. However, in that case, expression is coordinated rather than mutually exclusive, with all parasite lines analysed so far expressing either none or both of the genes (with the exception of parasite lines in which one of the genes is missing) [14–16,25]. The contiguous genes *PfRh4* and *eba-165* also seem to be co-regulated [4,20].

This complex picture reveals the existence of multiple different ways of regulation of the expression of genes encoding *P. falciparum* erythrocyte invasion proteins. Although the pattern of silenced and expressed genes may be very different in parasites living in the context of a host with acquired immune responses, our results on culture-adapted parasite lines demonstrate the existence in *P. falciparum* of the molecular machinery for the silencing of these genes in addition to the life cycle–dependent silencing common to most *Plasmodium* genes [18]. Epigenetically transmitted transcriptional silencing of invasion-related genes together with a certain level of mosaicism in a parasite population provides an enormous flexibility and capacity to adapt rapidly to changing host environments by simple means of natural selection and stochastic, low-frequency switching on and off of the expression of these genes.

The biological role of variant expression of invasion-related genes is unknown, and we can only speculate about its possible functions. While targeted disruption of the invasion-related genes *eba-175* and *pfRh2b* resulted in changes in the invasion pathways used by the parasites where they were disrupted [15,26], the active or silent state of the variantly expressed genes described in this study was not associated with detectable differences in growth rates or in the invasion pathways used. Regardless of the combination of silenced and

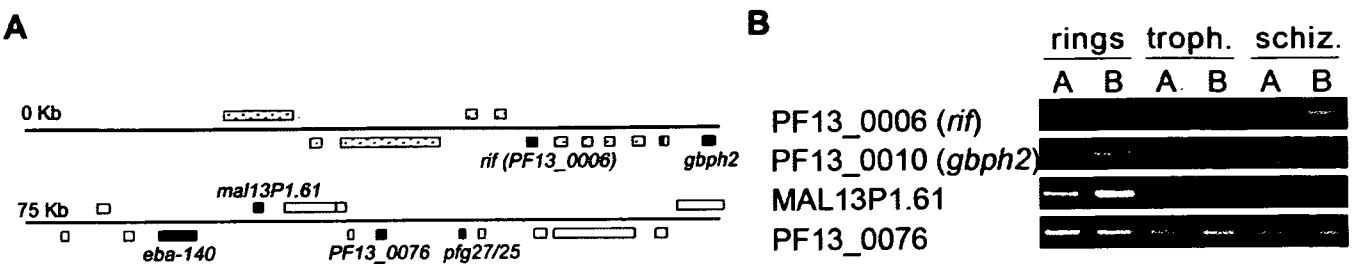

Figure 7. Expression of Genes Located in the Left Subtelomeric Region of Chromosome 13

(A) Schematic of the genes in the left end of Chromosome 13, as annotated in PlasmoDB. Genes above the line are transcribed towards the centromere, whereas genes below the line are transcribed towards the telomere. The genes analysed by RT-PCR are highlighted in grey, with their names. Members of the *var, rif,* and *stevor* families are spotted.

(B) RT-PCR analysis of RNA from rings, trophozoites, or schizonts of 3D7-A (lanes A) and 3D7-B (lanes B). The cDNA preparations used were the same as in Figure 5D. Thus, the controls for the amount of stage-specific cDNAs in Figure 5D also apply here.

doi:10.1371/journal.ppat.0030107.g007

expressed invasion-related genes, all 3D7-A subclones were able to invade using the neuraminidase- and trypsin-resistant receptor A [9], indicating that none of the genes found to vary in expression is responsible for this interaction. The identical invasion phenotype of all 3D7-A subclones suggests that the main force driving the variant expression of invasion-related genes is not the acquisition of the ability to invade different types of erythrocytes, but instead is immune evasion. This is a reasonable hypothesis, considering that in human populations diversity of the erythrocyte receptors

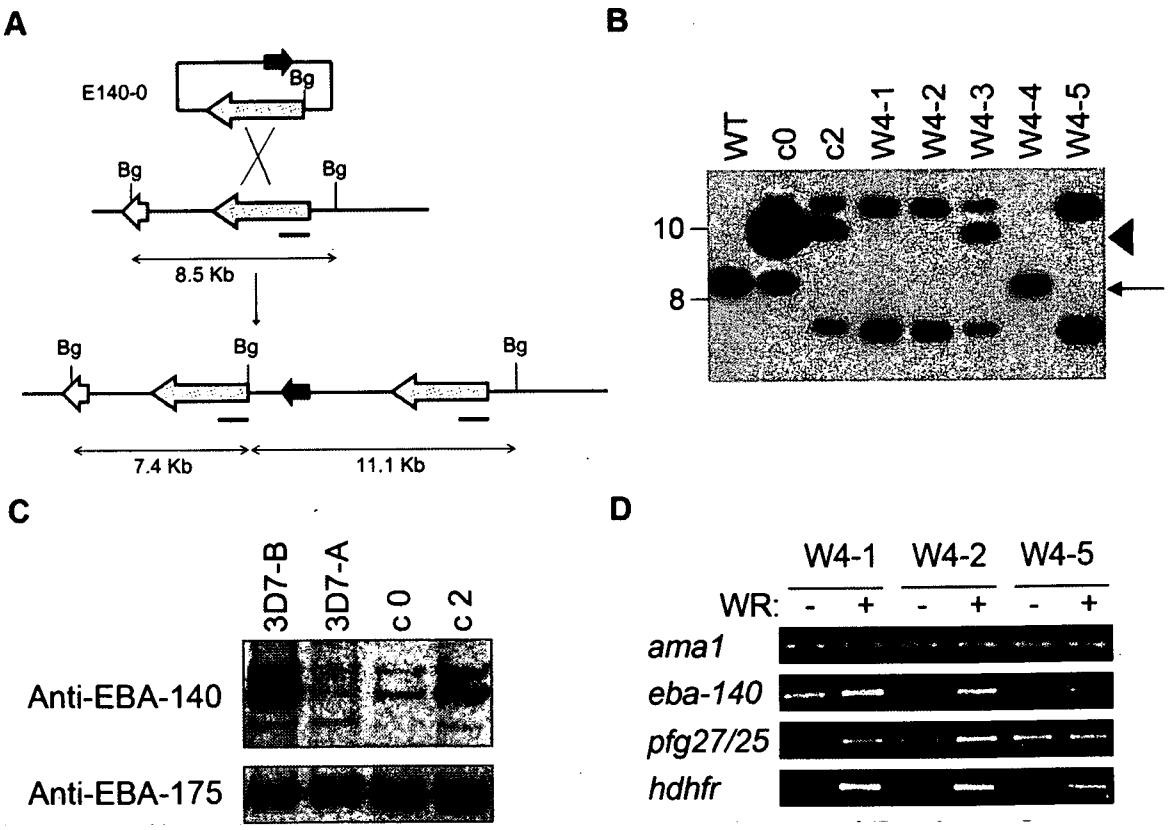

Figure 8. Activation of *eba-140* by Insertion of a Drug Resistance Marker in Its Vicinity

(A) Integration of the construct E140–0 (see Figure 5B) into the genomic *eba-140* locus. The *eba-140* and *hdhfr* genes are indicated by grey and black block arrows, respectively. The positions of the BglII sites (Bg) and the probe (line underneath the gene) used for the Southern blot analysis are indicated.

(B) Southern blot analysis of E140–0 transfected 3D7-A parasites. The lanes correspond to BglII-digested genomic DNA from wild-type 3D7-A (lane WT), 3D7-A transfected with E140–0 before (lane c0) or after two cycles on/off drug (lane c2), and five subclones of the latter (lanes W4–1 to W4–5). The arrow indicates the position of the band for the wild-type gene and the arrowhead the position of the episome (identical to the position of a band obtained by integration of multiple copies of the construct).

(C) Western blot analysis (as in Figure 2A) of schizonts extracts of 3D7-A, 3D7-B, and E140–0-transfected 3D7-A parasites before (lane c0) and after two cycles on/off drug (lane c2).

(D) RT-PCR analysis of schizonts from subclones that had been maintained for 1 mo either in the absence (lanes −) or the presence (lanes +) of WR99210 drug (increasing concentrations from 10 to 40 nM). The single-copy gene *ama1* was used to control the amount of stage-specific cDNA.

doi:10.1371/journal.ppat.0030107.g008

that the parasite uses for invasion is somehow limited, whereas merozoites are exposed to protective immune responses that are extremely diverse between different hosts. However, when silencing affects other invasion-related genes like *eba-175* or occurs in other genetic backgrounds, it will clearly affect the types of erythrocytes susceptible to invasion. Epigenetic silencing of invasion-related genes is likely to be the mechanism behind switching between invasion pathways.

The number of genes in the invasion-related multigene families is small for a role in immune evasion, especially when compared with the size of well-characterised variantly expressed gene families such as the *var* genes in *P. falciparum* or the *vsg* genes in *Trypanosoma brucei*. However, all members of the *clag, eba,* and *pfRh* families are polymorphic to some extent, and in some cases polymorphism is the consequence of positive selection [27,28]. Polymorphism, which is well known to help the parasite escape immune responses, and variant expression based on a limited number of alternatives, may play additive or even synergistic roles in immune evasion. Variant expression has the potential to enhance the capacity of polymorphism to avoid immune responses by permitting selection of parasites that keep in a silenced state the multigene family members with polymorphic allelic forms that are better recognised by protective immune responses in a particular host.

In summary, we describe an additional layer of complexity of the process of erythrocyte invasion, showing that the parasite has multiple modes of controlling the expression of genes involved in this process. This may provide an advantage to the parasite in its constant race to escape the immune system of its human host.

Materials and Methods

Parasites, transfection, and subcloning. Parasite cultures were maintained under standard conditions in medium containing Albumax II. The parasite lines 3D7-A and 3D7-B are the same cloned parasite line 3D7 maintained in different laboratories for several years. Genotyping was used to confirm their 3D7 identity [9]. The subclones 4D, 6D, 10E, 10G, 1.2B, and 1.2F were originated by subcloning 3D7-A by limiting dilution [12]. The subclones W4-1 to W4-5 were obtained by subcloning by limiting dilution 3D7-A parasites that had been transfected with the plasmid E140-0 and went through two cycles on/off drug to promote integration of the plasmid (see Figure 8 and Results). Genotyping of the highly polymorphic gene *msp2* by HinfI restriction fragment length polymorphism (RFLP) [29] was used to confirm the 3D7 identity of all subclones and rule out contamination from other parasite lines (unpublished data). Details of the methods used for transfection and subcloning are provided in Text S1.

One-cycle FACS-based growth assay, erythrocyte digestions, and invasion assays. To determine the growth rate of different subclones of the parasite line 3D7-A, synchronised cultures of the different subclones were diluted with fresh erythrocytes to an approximate parasitaemia of 0.7% immediately after sorbitol lysis. After culturing for 15 to 20 h, when most of the parasites were at the late trophozoite or early schizont stage, parasitaemia was determined by FACS as described [30] (time 0) using a FACScalibur cytometer (Becton Dickinson, http://www.bd.com/). Parasitaemia was determined again by FACS 48 h later, and the growth rate determined as the ratio between the parasitaemia at the 48- and 0-h time points. Erythrocyte digestions and invasion assays were performed as described [9], with small modifications explained in Text S1.

Preparation of RNAs, reverse transcription, and semi-quantitative PCR. To obtain RNA for microarray or RT-PCR analysis, parasites were synchronised to a 5-h window by purifying schizonts from a culture with abundant late forms on 70% Percoll, and removing late forms by sorbitol lysis 5 h later. Parasites were then left undisturbed for 39 h and 30 min (3D7-A and subclones) or 41 h (3D7-B), and harvested in 20-erythrocyte pellet volumes of Trizol (Invitrogen, http://www.invitrogen.com/). These times were determined in preliminary experiments for each parasite line as the times at which 20% of the schizonts had burst (estimated from the ratio of rings to schizonts). RNA in Trizol was frozen at −70 °C and later purified according to the manufacturer's instructions. RNA was then treated with RNAse-free DNAse I (Qiagen, http://www.qiagen.com/) and cleaned with the RNeasy MinElute cleanup kit (Qiagen). cDNA was obtained by reverse transcribing 0.5 μg of total RNA using the AMV reverse transcription kit (Promega, http://www.promega.com/) with oligo dT primers. To rule out the possibility of gDNA contamination, parallel reactions were performed for all samples in the absence of reverse transcriptase and tested by PCR with at least two primer pairs. To achieve semi-quantitative conditions, PCR was performed for only 25 cycles, and the amount of starting cDNA was adjusted for each primer pair to obtain bands that were clearly visible but not saturating. Single-copy genes with similar timing of expression [18,19] to the genes under analysis were used to control the amount of cDNA specific of each stage. All of the primers used in this study are described in Dataset S2.

Microarray analysis. The Affymetrix PFSANGER array (http://www.affymetrix.com/) was used for these experiments. Details of the array, experimental procedure, RMA normalization, and data analysis are available in Text S1.

Plasmids and antibodies. The procedure used for the construction of the plasmids E140–0, E140–800, and E-140-1300 (Figure 5B) is explained in Text S1. The antibodies used in this study and their sources are also described in Text S1.

Preparation of schizont extracts, culture supernatants, and metabolic labelling of parasites. Schizont extracts for western blot were prepared by resuspending pellets of Percoll-purified schizonts into 20-pellet volumes of PBS, adding 40-pellet volumes of 2x SDS protein loading buffer and heating for 5 min at 95 °C before storing at −70 °C until use. NP-40 extracts of schizonts for immunoprecipitation were prepared approximately as described [14]. To obtain culture supernatants, tightly synchronised parasite cultures with abundant segmented schizonts were enriched for schizont-infected erythrocytes by gelatin flotation. Schizont-enriched fractions (typically 80% parasitaemia) were placed back in culture at a haematocrit of approximately 0.3% and supernatants harvested by centrifugation 13 to 20 h later. For the preparation of supernatants in Albumax-free medium, it was critical that the original culture only contained very mature forms, because otherwise it resulted in death of the parasites before rupture and under-representation of some of the proteins usually released into the culture supernatant (unpublished data). Metabolic labelling of parasites was achieved approximately as described [14].

Fractionation of culture supernatants and mass spectrometry. Concentrated culture supernatants (from 5 ml of original supernatant) prepared in the absence of Albumax were loaded into a Q-Sepharose column in 0.5x PBS buffer. After washing with 0.5x PBS + 0.1 M NaCl, elution was performed with 0.5x PBS + 0.25 M NaCl. This fractionation resulted in a significant enrichment in the proteins of interest and elimination of haemoglobin. For mass spectrometry, fractions containing the proteins of interest were concentrated and resolved in 20 cm 5.5% polyacrylamide gels. The bands of interest were excised, reduced, alkylated, and trypsin-digested, then the released peptides were processed for mass spectrometry and analysed in a Reflex III MALDI-ToF mass spectrometer (Bruker Daltonics, http://www.bdal.de/). Data were analysed using Mascot software (Matrix Science, http://www.matrixscience.com/). Analysis of an excision in the 3D7-B lane corresponding to the position of Clag3.2 yielded no signal.

SDS-PAGE, western blot, immunoprecipitation, erythrocyte binding assays, and immunofluorescence assays. Details of the procedures used for these experiments are available in Text S1.

Supporting Information

Dataset S1. Microarray Comparison of 3D7-A and 3D7-B

Expression values for the 5,685 genes of *P. falciparum* analysed on the PFSANGER microarray, normalised, and logged (base 2) values (columns 2–5). The values provided for each gene (in rows) are the Log2 Ratio (column 6) of the contrast 3D7-B versus 3D7-A, followed by the moderated *t*-stats (column 7 = t), *p*-values (column 8 = P.Value), adjusted *p*-values for multiple correction (column 9 = adj.P.Value), and B statistics or log Odds (column 10 = B) as given by the function "topTable" in the Limma package of Bioconductor (http://www.bioconductor.org/packages/1.9/bioc/html/limma.html).

Found at doi:10.1371/journal.ppat.0030107.sd001 (1.1 MB XLS).

Dataset S2. Details of the Primers Used in This Study

PlasmoDB accession numbers (systematic gene names/IDs) for the genes mentioned in this article are also described in this dataset.

Found at doi:10.1371/journal.ppat.0030107.sd002 (28 KB XLS).

Figure S1. RT-PCR Analysis of 3D7-A Subclones

(A) Stability of the patterns of expression of *clag* genes. RNA from tightly synchronised schizonts of the subclones W4–1, W4–2, and W4–5 was prepared after maintaining the parasites in culture for an additional 32 d after they were harvested to prepare the RNA used in Figure 4. The pattern of expression remained identical (compare with Figure 4A). These parasite lines had been cultured for almost 2 mo since cloning, indicating that silencing or expression of these genes is stably clonally transmitted for at least 25–30 cycles of division.
(B) RT-PCR analysis of *pfRh* genes in two subclones of each of the two groups that were analysed in separate experiments in Figure 4. Expression can be compared here among these four subclones. W4–1 and W4–2 (and by extension W4–3 and W4–4) express lower amounts of *pfRh2b* than 1.2B and 1.2F (and by extension 6D, 10E, and 10G), whereas expression of other members of the *pfRh* multigene family was similar among all the subclones.

Found at doi:10.1371/journal.ppat.0030107.sg001 (92 KB TIF).

Figure S2. Quantitative PCR Analysis of Expression of *clag3.1* and *clag3.2* in HB3 Parasites

P. falciparum HB3B line was derived from the cloned line HB3A by infecting chimpanzees through mosquito bite [13]. Both clones were obtained from David Walliker. It is important to note that parasite lines 3D7-A and 3D7-B [9] are unrelated to 3D7A and 3D7B described by Walliker and collaborators [13] and were given the same names by mistake. HB3B#1 and HB3B#2 correspond to stocks of HB3B produced on different dates. The subclones C6, F4, F5, and G11 were obtained by limiting dilution of HB3B#2. Real-time RT-PCR analysis was performed with QuantiTect SYBR Green (Qiagen) approximately as described [8] using RNA from relatively synchronised cultures harvested at the schizont stage. Results are expressed relative to expression of *rhoph2*, which is expressed with a similar timing.
pGEM-T easy plasmids containing each DNA fragment were used as standards. The amount of each plasmid standard was compensated by evaluating the relative amount using primers located on the plasmid backbone, SP6 primer (ATTTAGGTGACACTATAGAA) and pGEM.rtF (GCAGGTCGACCATATG). Primers for *clag3.1* and *clag3.2* were described previously [8]. Primers for *rhoph2* were GTAACAACACTTACTAAGGCAGACT and GTACAAAGCTACAATATTGTTAGATCT.
To rule out the possibility that gene conversion had occurred in some of the HB3-derived lines, the full ORF of *clag3.1* and *clag3.2* were PCR amplified from gDNA of HB3A and HB3B with primers located in the divergent 5′ and 3′ UTR regions and the regions used for quantitative PCR sequenced from these PCR products. The results ruled out the possibility that gene conversion was confounding the expression results (unpublished data).

Found at doi:10.1371/journal.ppat.0030107.sg002 (39 KB TIF).

Figure S3. RT-PCR Analysis of RNA from Parasites Selected for Growth in Different Erythrocyte Types

To test the possibility that expression or silencing of certain invasion-related genes might provide only a small selective advantage for the invasion of neuraminidase plus trypsin–treated erythrocytes that escaped detection by standard invasion assays, we selected 3D7-A parasites for growth in these erythrocytes. Furthermore, to test the possibility that the expression status of these genes affected the capacity to invade erythrocytes of different ages, we selected 3D7-A parasites for growth in ageing erythrocytes.
3D7-A parasites were grown in parallel in untreated (lanes Unt.) or neuraminidase plus trypsin–treated (lanes Nm.+Tr.) erythrocytes for four cycles and in fresh (stored for less than a week, always at 4 °C) or ageing (kept for at least one week at room temperature) erythrocytes during eight cycles. Parasites were then grown in fresh untreated erythrocytes to obtain enough parasite material for RNA isolation. RNA from tightly synchronised schizonts was obtained and the expression of invasion-related genes tested by semi-quantitative PCR. The single-copy genes *rhoph2* and *ama1* were used to control the amount of stage-specific cDNA as in Figure 4.
This analysis did not reveal any difference in the balance between *clag3.1* and *clag3.2* or in the expression of any of the other genes tested between the selected and control cultures, with the exceptions of *pfRh2b* and *pfRh4*, which were expressed at lower levels in cultures grown in ageing erythrocytes. This result suggests that these ligands may not be used to invade senescent erythrocytes.
Direct invasion assays did not reveal any major difference among 3D7-A subclones in their capacity to invade ageing erythrocytes, which were invaded at around 30% the rate for fresh erythrocytes (unpublished data).

Found at doi:10.1371/journal.ppat.0030107.sg003 (208 KB TIF).

Figure S4. Chromosomal Position of Invasion-Related Multigene Families

Information was obtained from PlasmoDB (http://www.plasmodb.org/). The position of *clag8* (MAL7P1.229) is indicated with a question mark because it is located in the left subtelomeric region of Chromosome 7 according to PlasmoDB but was experimentally assigned to Chromosome 8 [8]. The majority of genes of invasion-related multigene families that exhibited variant expression (*eba*, *pfRh*, and *clag* families) are located in subtelomeric positions, with the exception of *pfRh2a* and *pfRh2b*, which are located relatively near the centromere. The *acbp* multigene family, of which one gene was also found to vary in expression but for which a role in the process of invasion has not been established, is also located in subtelomeric positions, with the exception of the *acbp* gene in Chromosome 8.

Found at doi:10.1371/journal.ppat.0030107.sg004 (21 KB TIF).

Text S1. Supporting Text

Online supporting materials and methods, discussion, and references.

Found at doi:10.1371/journal.ppat.0030107.sd003 (36 KB PDF).

Accession Numbers

Microarray data have been deposited with ArrayExpress under accession number E-SGRP-9. The PlasmoDB (http://www.plasmodb.org/plasmo/home.jsp) accession numbers (systematic gene names/IDs) for the genes mentioned in this article are described in Dataset S2.

Acknowledgments

We are grateful to S. A. Howell for the MALDI-TOF analysis and to I. Ling and E. Knuepfer for helpful discussion and for providing some reagents. We are also grateful to L. Ribas de Pouplana for providing lab space to perform some of the experiments and for critical reading of the manuscript. We thank MR4 for providing antibodies contributed by J. H. Adams.

Author contributions. AC and AAH conceived and designed the experiments. AC, CC, and OK performed the experiments. AC and CC analyzed the data. AC, BYSYL, and AI contributed reagents/materials/analysis tools. AC wrote the paper. AAH obtained funding for the study.

Funding. This work was funded in part by the UK Medical Research Council, The Wellcome Trust Malaria Functional Genomics Initiative (ref. 066742), the European Union (through the BioMalPar Network of Excellence), and a grant from the US National Institutes of Health (HL078826). BYSYL was funded by a UK Medical Research Council PhD Studentship.

Competing interests. The authors have declared that no competing interests exist.

References

1. Aikawa M, Miller LH, Johnson J, Rabbege J (1978) Erythrocyte entry by malarial parasites. A moving junction between erythrocyte and parasite. J Cell Biol 77: 72–82.
2. Cowman AF, Crabb BS (2006) Invasion of red blood cells by malaria parasites. Cell 124: 755–766.
3. Sim BK, Chitnis CE, Wasniowska K, Hadley TJ, Miller LH (1994) Receptor and ligand domains for invasion of erythrocytes by *Plasmodium falciparum*. Science 264: 1941–1944.
4. Stubbs J, Simpson KM, Triglia T, Plouffe D, Tonkin CJ, et al. (2005) Molecular mechanism for switching of *P. falciparum* invasion pathways into human erythrocytes. Science 309: 1384–1387.
5. Baum J, Pinder M, Conway DJ (2003) Erythrocyte invasion phenotypes of *Plasmodium falciparum* in The Gambia. Infect Immun 71: 1856–1863.
6. Okoyeh JN, Pillai CR, Chitnis CE (1999) *Plasmodium falciparum* field isolates

commonly use erythrocyte invasion pathways that are independent of sialic acid residues of glycophorin A. Infect Immun 67: 5784–5791.
7. Ling IT, Florens L, Dluzewski AR, Kaneko O, Grainger M, et al. (2004) The *Plasmodium falciparum clag9* gene encodes a rhoptry protein that is transferred to the host erythrocyte upon invasion. Mol Microbiol 52: 107–118.
8. Kaneko O, Yim Lim BYS, Iriko H, Ling IT, Otsuki H, et al. (2005) Apical expression of three RhopH1/Clag proteins as components of the *Plasmodium falciparum* RhopH complex. Mol Biochem Parasitol 143: 20–28.
9. Cortés A, Benet A, Cooke BM, Barnwell JW, Reeder JC (2004) Ability of *Plasmodium falciparum* to invade Southeast Asian ovalocytes varies between parasite lines. Blood 104: 2961–2966.
10. Mayer DC, Kaneko O, Hudson-Taylor DE, Reid ME, Miller LH (2001) Characterization of a *Plasmodium falciparum* erythrocyte-binding protein paralogous to EBA-175. Proc Natl Acad Sci USA 98: 5222–5227.
11. Lobo CA, Fujioka H, Aikawa M, Kumar N (1999) Disruption of the *Pfg27* locus by homologous recombination leads to loss of the sexual phenotype in *P. falciparum*. Mol Cell 3: 793–798.
12. Cortés A (2005) A chimeric *Plasmodium falciparum Pfnbp2b/Pfnbp2a* gene originated during asexual growth. Int J Parasitol 35: 125–130.
13. Walliker D, Quakyi IA, Wellems TE, McCutchan TF, Szarfman A, et al. (1987) Genetic analysis of the human malaria parasite *Plasmodium falciparum*. Science 236: 1661–1666.
14. Taylor HM, Grainger M, Holder AA (2002) Variation in the expression of a *Plasmodium falciparum* protein family implicated in erythrocyte invasion. Infect Immun 70: 5779–5789.
15. Duraisingh MT, Triglia T, Ralph SA, Rayner JC, Barnwell JW, et al. (2003) Phenotypic variation of *Plasmodium falciparum* merozoite proteins directs receptor targeting for invasion of human erythrocytes. EMBO J 22: 1047–1057.
16. Nery S, Deans AM, Mosobo M, Marsh K, Rowe JA, et al. (2006) Expression of *Plasmodium falciparum* genes involved in erythrocyte invasion varies among isolates cultured directly from patients. Mol Biochem Parasitol 149: 208–215.
17. Bethke LL, Zilversmit M, Nielsen K, Daily J, Volkman SK, et al. (2006) Duplication, gene conversion, and genetic diversity in the species-specific acyl-CoA synthetase gene family of *Plasmodium falciparum*. Mol Biochem Parasitol 150: 10–24.
18. Le Roch KG, Zhou Y, Blair PL, Grainger M, Moch JK, et al. (2003) Discovery of gene function by expression profiling of the malaria parasite life cycle. Science 301: 1503–1508.
19. Bozdech Z, Llinas M, Pulliam BL, Wong ED, Zhu J, et al. (2003) The transcriptome of the intraerythrocytic developmental cycle of *Plasmodium falciparum*. PLoS Biol 1: e5. doi:10.1371/journal.pbio.0000005.
20. Gaur D, Furuya T, Mu J, Jiang LB, Su XZ, et al. (2006) Upregulation of expression of the reticulocyte homology gene 4 in the *Plasmodium falciparum* clone Dd2 is associated with a switch in the erythrocyte invasion pathway. Mol Biochem Parasitol 145: 205–215.
21. Scherf A, Hernandez-Rivas R, Buffet P, Bottius E, Benatar C, et al. (1998) Antigenic variation in malaria: in situ switching, relaxed and mutually exclusive transcription of *var* genes during intra-erythrocytic development in *Plasmodium falciparum*. EMBO J 17: 5418–5426.
22. Duraisingh MT, Voss TS, Marty AJ, Duffy MF, Good RT, et al. (2005) Heterochromatin silencing and locus repositioning linked to regulation of virulence genes in *Plasmodium falciparum*. Cell 121: 13–24.
23. Freitas-Junior LH, Hernandez-Rivas R, Ralph SA, Montiel-Condado D, Ruvalcaba-Salazar OK, et al. (2005) Telomeric heterochromatin propagation and histone acetylation control mutually exclusive expression of antigenic variation genes in malaria parasites. Cell 121: 25–36.
24. Frank M, Dzikowski R, Costantini D, Amulic B, Berdougo E, et al. (2006) Strict pairing of *var* promoters and introns is required for var gene silencing in the malaria parasite *Plasmodium falciparum*. J Biol Chem 281: 9942–9952.
25. Triglia T, Duraisingh MT, Good RT, Cowman AF (2005) Reticulocyte-binding protein homologue 1 is required for sialic acid-dependent invasion into human erythrocytes by *Plasmodium falciparum*. Mol Microbiol 55: 162–174.
26. Reed MB, Caruana SR, Batchelor AH, Thompson JK, Crabb BS, et al. (2000) Targeted disruption of an erythrocyte binding antigen in *Plasmodium falciparum* is associated with a switch toward a sialic acid-independent pathway of invasion. Proc Natl Acad Sci USA 97: 7509–7514.
27. Rayner JC, Tran TM, Corredor V, Huber CS, Barnwell JW, et al. (2005) Dramatic difference in diversity between *Plasmodium falciparum* and *Plasmodium vivax* reticulocyte binding-like genes. Am J Trop Med Hyg 72: 666–674.
28. Verra F, Chokejindachai W, Weedall GD, Polley SD, Mwangi TW, et al. (2006) Contrasting signatures of selection on the *Plasmodium falciparum* erythrocyte binding antigen gene family. Mol Biochem Parasitol 149: 182–190.
29. Felger I, Tavul L, Beck HP (1993) *Plasmodium falciparum:* A rapid technique for genotyping the merozoite surface protein 2. Exp Parasitol 77: 372–375.
30. Persson KE, Lee CT, Marsh K, Beeson JG (2006) Development and optimization of high-throughput methods to measure *Plasmodium falciparum*-specific growth inhibitory antibodies. J Clin Microbiol 44: 1665–1673.

OPEN ACCESS Freely available online PLoS one

A Novel DBL-Domain of the *P. falciparum* 332 Molecule Possibly Involved in Erythrocyte Adhesion

Kirsten Moll[1,2], Arnaud Chêne[1,2,3☯], Ulf Ribacke[1,2☯], Osamu Kaneko[4], Sandra Nilsson[1,2], Gerhard Winter[1,2], Malin Haeggström[1,2], Weiqing Pan[5], Klavs Berzins[6], Mats Wahlgren[1,2], Qijun Chen[1,2*]

1 Department of Parasitology, Mycology and Environmental Microbiology (PMV), Swedish Institute for Infectious Disease Control (SMI), Karolinska Institutet, Stockholm, Sweden, 2 Department of Microbiology, Tumour and Cell Biology (MTC), Karolinska Institutet, Stockholm, Sweden, 3 Center for Infectious Medicine (CIM), Karolinska Institutet, Stockholm, Sweden, 4 Department of Molecular Parasitology, Ehime University Graduate School of Medicine, Ehime, Japan, 5 Department of Etiologic Biology, Second Military Medical University, Shanghai, China, 6 Department of Immunology, Wenner-Gren Institute, Stockholm University, Stockholm, Sweden

Plasmodium falciparum malaria is brought about by the asexual stages of the parasite residing in human red blood cells (RBC). Contact between the erythrocyte surface and the merozoite is the first step for successful invasion and proliferation of the parasite. A number of different pathways utilised by the parasite to adhere and invade the host RBC have been characterized, but the complete biology of this process remains elusive. We here report the identification of an open reading frame (ORF) representing a hitherto unknown second exon of the Pf332 gene that encodes a cysteine-rich polypeptide with a high degree of similarity to the Duffy-binding-like (DBL) domain of the erythrocyte-binding-ligand (EBL) family. The sequence of this DBL-domain is conserved and expressed in all parasite clones/strains investigated. In addition, the expression level of Pf332 correlates with proliferation efficiency of the parasites *in vitro*. Antibodies raised against the DBL-domain are able to reduce the invasion efficiency of different parasite clones/strains. Analysis of the DBL-domain revealed its ability to bind to uninfected human RBC, and moreover demonstrated association with the iRBC surface. Thus, Pf332 is a molecule with a potential role to support merozoite invasion. Due to the high level of conservation in sequence, the novel DBL-domain of Pf332 is of possible importance for development of novel anti-malaria drugs and vaccines.

Citation: Moll K, Chêne A, Ribacke U, Kaneko O, Nilsson S, et al (2007) A Novel DBL-Domain of the *P. falciparum* 332 Molecule Possibly Involved in Erythrocyte Adhesion. PLoS ONE 2(5): e477. doi:10.1371/journal.pone.0000477

INTRODUCTION

The invasion of RBC by a *Plasmodium*-merozoite is a cascade like process involving adhesion, reorientation, junction-formation and invagination. This procedure requires close interaction between the parasite derived ligands and the host receptors on the RBC surface (reviewed by Gaur et al. [1]). Interestingly, a majority of *Plasmodium falciparum* merozoites released from ruptured schizonts fail to invade new RBC *in vitro*. Further, *P. falciparum* purified merozoites do not consistently infect RBC [2,3] while in contrast isolated merozoites of both murine and primate malaria parasites easily invade and proliferate within new RBC [3]. It has therefore been speculated that parasite derived molecules adhering to the merozoites are essential elements facilitating the invasion process [4] or that a specific interaction between infected and uninfected RBC prior to invasion may be necessary [5].

P. falciparum displays numerous parasite derived proteins on the merozoite surface that fulfil important functions for the multiplication of the parasite; the most important ones characterized so far are the Merozoite surface protein 1 (MSP-1) and the Apical membrane protein 1 (AMA-1), which are essential for the parasites survival [6,7]. During the invasion process, the parasite forms a tight junction with the RBC membrane involving several proteins discharged from micronemes and rhoptries in the apical part of the cell. Among these are the erythrocyte binding proteins of the EBL-family located in the micronemes and the reticulocyte binding like (RBL) proteins situated at the neck of the rhoptries, which are expressed simultaneously by the merozoite. However, it is probably the available receptor on the RBC surface that determines which ligand the parasite employs for invasion [8].

EBA-175 was the first protein identified to be involved in the junction formation between merozoite and RBC mediating binding to the receptor glycophorin A (reviewed by Gaur et al. [1]), followed by EBA-175 paralogues such as EBA-140 and EBA-181 binding to glycophorin C or unknown receptors [9]. All members of the EBA-family are featured by an N-terminal signal sequence followed by a cysteine-rich motif with one or two Duffy-binding like domains, a C-terminal cysteine-rich motif, a transmembrane (TM) domain and a short cytoplasmic tail. Parasite mutants deficient in single members of the EBA-family do not show a significantly reduced merozoite invasion rate, as demonstrated by BAEBL/EBA-140 or JESEBL/EBA-180 knockout clones that maintain a comparable RBC invasion rate as wild type parasites [10,11]. However, single amino acid alterations in the EBA-140 or EBA-181 sequences will lead to a change in receptor specificity, while sequence polymorphism in EBA-175 does not change its receptor-binding specificity [10].

A recent study by Glushakova [12] illustrates that merozoites invade RBC more efficiently when the iRBC are bound to uninfected RBC prior to schizont rupture and merozoite release.

Academic Editor: Mauricio Rodrigues, Federal University of São Paulo, Brazil

Received February 26, 2007; **Accepted** May 3, 2007; **Published** May 30, 2007

Funding: This work was funded by grants from the European Malaria Consortium (BioMalPar), the Swedish Research Council (348-2003-4845), SIDA/SAREC (SWE-2003-241).

Competing Interests: The authors have declared that no competing interests exist.

* **To whom correspondence should be addressed.** E-mail: Qijun.Chen@smi.ki.se

☯ These authors contributed equally to this work.

Molecules that participate in this interaction between iRBC and RBC may likewise play an important role in the initial adhesion process between merozoite and RBC [9]. A candidate molecule mediating the interaction between late stage iRBC and RBC is the polypeptide Pf332 (Antigen 332), which was first identified by Mercereau-Puijalon [13,14]. Pf332 is highly glutamic acid rich and contains long repetitive sequences in an internal region named EB200, and a conserved tryptophan-rich domain (WRD) with similarities to that of PfEMP-1, SURFIN, and PkSICAvar [4]. Antibodies targeting this region can block the adhesion of iRBC to cells expressing CD36 and efficiently inhibit parasite invasion [15–17]. However, antibodies to the glutamic-acid reach repeats cross-react with several other *P. falciparum* proteins including Pf11-1, RESA/Pf155 with similar repetitive sequences, and the specificity of its inhibitory effect has therefore not been conclusive. Recent studies suggest that Pf332 assembles together with a number of different surface-related proteins such as the RIFINs and PfEMP1 in the erythrocyte-cytoplasm to be directed together to the erythrocyte membrane [18] although the biological function of Pf332 has remained unclear.

Here we propose that the open reading frame of Pf332 as originally described [13,19] is in fact only the second exon of a giant gene comprising two exons. We identified a previously unrecognized Pf332 exon I, which is present in all parasite clones/strains investigated and encodes an erythrocyte-binding DBL-domain together with a transmembrane domain. Characterization of both the native and *in vitro* expressed Pf332 DBL-domain revealed its surface association and the ability to bind to human RBC. Significantly, antibodies raised against this region were able to reduce the invasion efficiency *in vitro* independent of geographical origin or receptor specificity of the *P. falciparum* clone/strain. This suggests the conserved polypeptide encoded by exon I of Pf332 exhibit a functional role during the RBC invasion process and is therefore a potential novel candidate for a blood stage vaccine.

RESULTS

The gene encoding Pf332 consists of two exons separated by a short intron

During a survey to identify open reading frames (ORF) containing domains able to bind to RBC, the ORF PF11_0506 was identified, for which the adjacent ORF PF11_0507 encoding Pf332 started only 280 bp after the predicted stop codon of PF11_0506. The length of the intergenic region is very short compared to the mean length in *P. falciparum* (1694 bp) [20] and was thus assumed to be an intron rather than an intergenic region.

PCR amplification from gDNA and cDNA of the 3D7AH1 parasite clone was performed using a set of primers, where the forward primer UP3 was located at the 3'end of PF11_0506 and the reverse primer UP4 at the 5'end of PF11_0507 (Pf332). The size of the RT-PCR products from cDNA was 350 bp (Fig. 1A), whereas the size of the PCR products was 600 bp if gDNA of the clones 3D7AH1 (Fig. 1B) or FCR3S1.2 (data not shown) were used as a template. Comparison of the sequences of the PCR and RT-PCR products revealed an intron sequence possessing typical 'gt-ag' splicing sites at its ends.

To further confirm that the two transcripts of PF11_0506 and PF11_0507 constitute a single mRNA, Northern blot hybridisations were performed with two different probes. Probe 1 was located at 5'-end of PF11_0506 (amplified with UP1 and UP2, Fig 1A), while probe 2 covered the splicing sites (amplified with UP3 and UP4, Fig 1A). RNA was purified from the 3D7AH1 clone at around 20 h post invasion (p.i.). The two probes hybridised to a single transcript of a size considerably higher than 9.4 kb (Fig. 1C).

Combining these data, it can be concluded that the two ORFs (PF11_0506 and PF11_0507) annotated in the 3D7 genome database, as distinct genes are actually two exons of a single gene encoding Pf332. The full size of the mRNA (3D7AH1) is 18282 bp encoding a polypeptide of 6094 amino acids with a predicted molecular weight of approximately 670 kDa.

The sequence of exon I of Pf332 is conserved in *P. falciparum*

A single DNA fragment was amplified from 10 different *P. falciparum* clones/strains originally isolated from various geographical locations and one Ugandan patient isolate. PCR amplification was conducted with a pair of primers (UP1, UP5) specific to the sequence of the 3D7AH1 clone (Fig. 1A and Fig. S1). When digested with the restriction enzyme EcoR I (3 digestion sites are present in the 3D7AH1 sequence, data not shown) the PCR products did not show any restriction fragment length polymorphism (data not shown). In addition, the DNA fragments of 11 parasite clones/strains (3D7AH1, NF54, FCR3S1.2, TM284S2, Dd2, FCB-3, K1, R29, FCR3CSA, F32 and UAS22) encoded by exon I of the molecule were sequenced and only four point mutations were found (in K1, 3D7AH1 and Dd2; Table 1). In contrast, sequence polymorphism was mainly reported in the repetitive region of exon II [14], as often seen in molecules important during sporozoite and merozoite invasion such as the repetitive regions of the circumsporozoite protein (CSP) and the block two sequence of MSP-1.

Exon I of Pf332 encodes for a DBL-domain with high similarity to the DBL-domains of the EBL-protein family

BLASTP search and sequence alignment of the amino acid sequence encoded by the ORF PF11_0506 revealed that the N-terminal region (aa 1-250) possesses a domain homologous to the DBL-domains of the EBL-family including e.g. the EBA-175 of *P. falciparum* (Fig. S2) [21], although the overall protein structure of Pf332 differs from this protein family. Pf332 does neither contain a N-terminal segment (NTS) nor a signal leader sequence upstream of the DBL-domain (Fig. 2). The DBL-domains of the other EBL-family members are located further to the centre of the molecule, downstream of a NTS of variable size. Further, all EBL-family proteins presented an N-terminal signal peptide sequence.

Sequence comparison of the EBL-family proteins and the Pf332 showed that they share conserved cysteine residues and other amino acid residues, which are of importance for maintaining the structure of the molecule. Among 12 Cysteine-residues 5 are conserved indicating the formation of at least two disulfide bonds within the molecule (Fig. S2). The DBL-domain of Pf332 is more similar to the F2 than to the F1 region of the EBA-175 protein (Fig. 2); however, the absence of the WWXXXXXXXW sequence motif commonly found in other EBL family members suggests a distinct RBC-binding function for this domain.

Alignment with the EBL-family also reveals that Pf332 does not have a C-terminal Cysteine-rich domain after the DBL-domain. In contrast, Pf332 has a putative transmembrane region, located close to the DBL-domain (aa 540–560) (Fig. 2). Four membrane targeting motifs (RxLxE/Q) were found in the N-terminal region (aa 77–81), in the middle (aa 2628–2632) and close to the end (aa 4537–4541, 4922–4926) of the molecule, indicating that Pf332 is a transmembrane protein with a similar

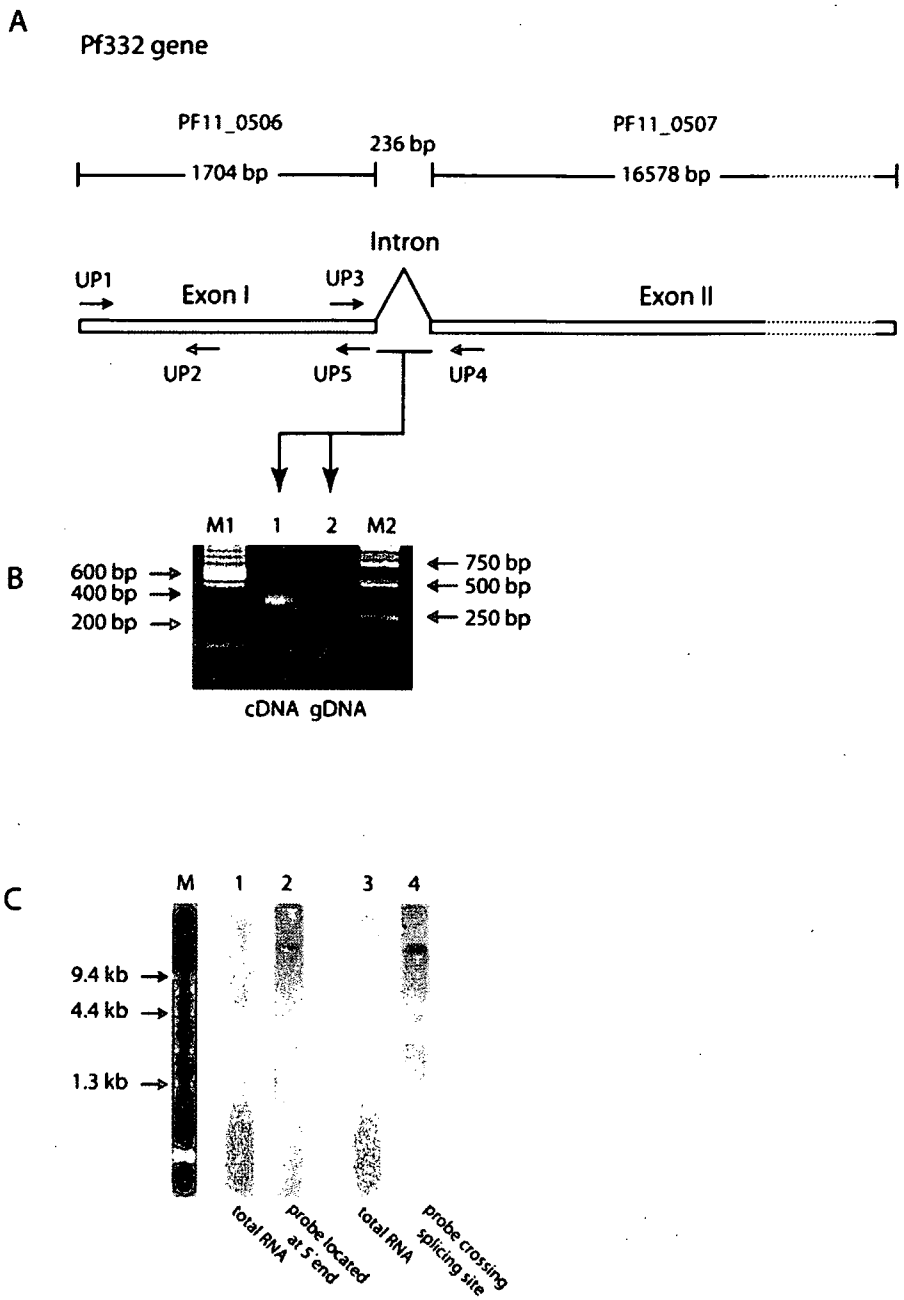

Figure 1. Structural analysis of the gene encoding Pf332. A. Schematic structure of the Pf332 gene. The gene is composed of a 5′ exon I (PF11_0506) with a size of 1704 bp and a 3′ exon II (PF11_0507), separated by a short intron of 236 bp. The 3′-exon II is the gene fragment previously referred to as the gene coding for the antigen Pf332. The location of the primers is indicated as arrows. **B.** PCR amplification from cDNA and gDNA across the intron region of the Pf332 gene: Lane 1: PCR amplification with primers UP3 and UP4 from cDNA; lane 2: PCR amplification with the same primer pair from gDNA. **C.** Northernblot with probes located at 5′-end (UP1–UP2) and across the splicing site (UP3–UP4) of the Pf332 gene. Total RNA from 3D7AH1 iRBC was resolved in an agarose gel (lanes 1 and 3). Lane 2 shows the hybridisation with the first probe (UP1–UP2); lane 4 shows the hybridisation with the second probe (UP3–UP4) revealing a band of the same size as seen in the first hybridization.
doi:10.1371/journal.pone.0000477.g001

transport pathway as other molecules directed to the surface, such as PfEMP1 [22,23].

Pf332 is expressed by all parasites studied

Microarray data illustrate that the transcription pattern of the Pf332 gene is similar in all investigated parasite clones/strains (HB3, 3D7, Dd2) [24,25]. This was confirmed by real-time quantitative PCR analysis using RNA of three parasite clones/strains (3D7AH1, FCR3S1.2, 7G8) collected every 4 hours from 8 h p.i. onwards. The primers used were specific to the 5′ region of the transcript. Transcription was normalized to *seryl-tRNA synthetase* as an internal standard control. Results (Fig. 3A) clearly showed that the gene encoding Pf332 is activated in all three parasite clones/strains at approximately 16 h reaching maximal transcription at 24 h p.i.. Although all parasite clones/strains displayed the same transcription pattern, the level of transcription varied considerably among the different clones/strains, with

Table 1. Amino acid substitutions in the region encoded by exon I of Pf332

Parasite clone/ strain	Position 69	Position 117	Position 329	Position 363
Dd2	Asn	Thr	Asn	*Thr*
FCR3S1.2	Asn	Thr	Asn	Met
FCB3	Asn	Thr	Asn	Met
F32	Asn	Thr	Asn	Met
K1	*Cys*	Thr	*Asp*	Met
UAS22	Asn	Thr	Asn	Met
TM284S2	Asn	Thr	Asn	Met
3D7AH1	Asn	*Ala*	Asn	Met

The amino acid residues of the consensus sequence of exon I of Pf332 are shown for 8 different parasite strains/clones, substitutions found in these sequences are visualized in italics.
doi:10.1371/journal.pone.0000477.t001

FCR3S1.2 iRBC showing a transcription rate twice as high as the 3D7AH1 and 7G8 iRBC (Fig. 3A).

In addition, Pf332 expression was investigated in 3D7AH1, FCR3S1.2 and 7G8 iRBC by immunofluorescence and Western blot analysis with antibodies specific to the N-terminal region (α-Pf332-DBL/nDBL) as compared to antibodies towards the repetitive region (EB200) of the molecule and the human monoclonal antibody m33G2 [16] (Fig. 3B, C and Fig. S3). Expression of Pf332 starts immediately after initiation of transcription [18] and reaches maximal levels at 36 h p.i.. Immunofluorescence with α-Pf332-DBL/nDBL sera visualized that the protein is found within the parasitophorous vacuole at the ring stage, while with maturation of the parasite it is transported through the iRBC cytoplasm and directed towards the surface of the host cell, as previously observed with sera against other regions of the molecule (Fig. 3B).

Further, FCR3S1.2 iRBC displayed a higher expression rate of Pf332 as compared to the two other strains (Fig. 3C) corresponding to the transcription patterns visualized by quantitative PCR. Interestingly, the parasite clone FCR3S1.2 has the fastest multiplication rate among the three clones/strains investigated, indicating that Pf332 might be a protein that supports the parasite invasion process.

The DBL-domain of Pf332 is surface associated and binds to human RBC *in vitro*

Immunofluorescence assays on live trophozoite iRBC (HB3, FCR3S1.2) at 36 to 40 h p.i. using a serum raised against the DBL-domain of Pf332 visualized that this domain is associated with the surface of the iRBC (Fig. 4 A–D). In order to exclude that the observed reactivity results from uptake of the antibody into the iRBC, respectively leaky membranes as often observed in late stage iRBC, IFA assays were in addition carried out with various control proteins, which are parasite-derived, but not exposed on the iRBC surface. Antibodies against the ATS-domain of PfEMP1, PfEMP2 as well as an unrelated control protein did not show any reactivity in these assays.

In order to investigate the function of the surface associated DBL-domain, recombinant proteins (tagged with Gluthatione-S-Transferase, GST) corresponding to either the DBL-domain (Pf332-DBL) or nonDBL-domain (Pf332-nDBL) (Fig. 5A) of Pf332 were generated in *E. coli.* These recombinant domains were assayed for their capacity to bind to human RBC. The Pf332-DBL-domain bound to the surface of human RBC, while neither the recombinant Pf332-nDBL-domain or an unrelated GST-tagged control protein showed any affinity to human RBC (Fig 5B). In additional experiments, receptors on the RBC surface were modified with different enzymes. Treatment of RBC with neuraminidase did not abolish the binding of the recombinant Pf332-DBL-domain suggesting that the receptor of Pf332 is not a glycophorin molecule, likewise treatment of the RBC with trypsin or heparitinase did not influence the binding of the Pf332-DBL-domain (data not shown).

To further illustrate the binding capacity of the DBL-domain, CHO cells transiently expressing the DBL- or the nDBL-domain on their surface were constructed and tested for their ability to bind to human RBC. After transfection, 30–35% of the CHO cells were positive for expression of the different domains. The cells presenting the Pf332-DBL-domain were found to have RBC attached to their surface, while the presence of either the Pf332-

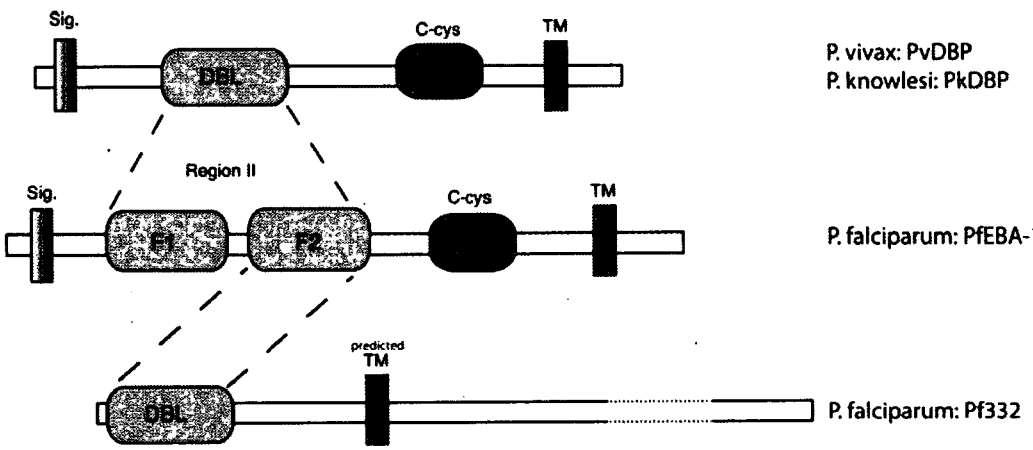

Figure 2. Schematic illustration of the conserved structure of the erythrocyte-binding region of Pf332 and the EBL family. The N-terminal region of the Pf332 encoded by exon I contains a Duffy-binding like domain homologous to the DBL-domain of the EBL-family. This domain of Pf332 is located closer to the N-terminal part of the molecule and lacks a signal leading sequence as compared to the other EBL family members. It aligns with the F2 region of EBA-175 of P. falciparum and the DBP of P. vivax. In addition, the carboxyl cysteine (c-cys)-rich domain present upstream of the transmembrane domain in EBA-175 and DBP is not found in Pf332.
doi:10.1371/journal.pone.0000477.g002

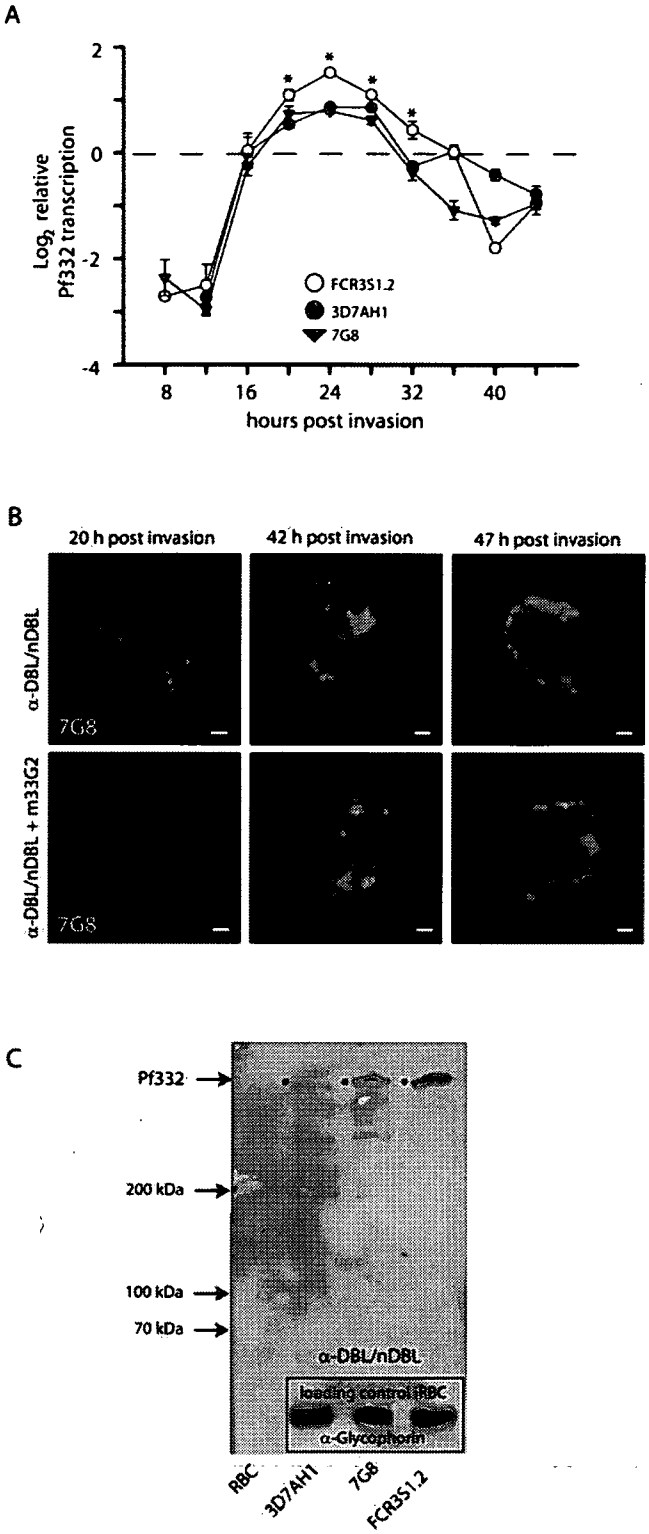

Figure 3. Transcription and expression of Pf332 in different P. falciparum clones/strains. A: The level of Pf332 mRNA transcription, relative to the endogenous control seryl-tRNA synthetase, was determined by real-time quantitative PCR. Normalized Pf332 levels at different times p.i. are plotted for 3D7AH1 (•), FCR3S1.2 (○) and 7G8 (▼). Error bars represent the standard deviation of the quotient and * denotes significantly higher levels of transcription in FCR3S1.2 ($p<0.001$, One Way ANOVA with Tukey test). The amount of Pf332 mRNA transcripts in FCR3S1.2 is around two fold higher than in 3D7AH1 and 7G8 at the time of maximal transcription. **B:** Upper panel: Immunofluorescence staining with α-DBL/nDBL-domain antibodies of Pf332. α-DBL/nDBL-domain antibodies (green) visualize at early trophzoite stage (around 20 h p.i.) vesicles that carry Pf332 in the cytosol of the iRBC; when the iRBC reaches late trophozoite/schizont stage (40–47 h p.i.), Pf332 can be observed in association with the iRBC membrane. Lower panel: Additional staining with the α-Pf332 monoclonal antibody m33G2. Staining with previously raised sera against the Pf332 (m33G2, red) show that α-DBL/nDBL-domain antibodies (green) co-localize with sera raised against the polypeptide encoded by exon II of Pf332. Staining is shown for the parasite strain 7G8, DNA staining with Hoechst (blue); Scale bars = 1 μm. **C:** Immunoblot analysis confirmed that antibodies raised against the DBL/nDBL-domain of Pf332 reacted with the same high molecular weight polypeptide as the previously raised antibodies α-EB200 and m33G2 (compare Fig. S3). This verifies that the sequence of the Pf332-DBL/nDBL-domain is an additional exon of the same open reading frame as the previously described Pf332. The total amount of expressed Pf332 varies in between parasites, with FCR3S1.2 iRBC expressing the highest amount of Pf332. An α-glycophorin antibody was used compare the amount of loaded material in the different lanes. The bands corresponding to Pf332 are marked with an asterix.

doi:10.1371/journal.pone.0000477.g003

nDBL-domain or MOCK transfection did not result in any RBC binding activity (Fig. 5C).

Antibodies against Pf332 decrease parasite invasion efficiency

Invasion inhibition assays in which late stage parasites were grown in the presence of α-Pf332-DBL/nDBL-antibodies visualized the influence of Pf332 on parasite invasion. For the three different parasite clones/strains FCR3S1.2, 3D7AH1 and 7G8, the antibodies showed an inhibition effect on invasion, with reduction to around 60% observed at concentrations of 1 mg/ml (Fig. 6), this effect was declining with decreasing concentrations of the α-Pf332-DBL/nDBL-antibodies. Antibodies against MSP-1 and AMA-1, known antigens involved in RBC invasion [6,7] revealed a similar inhibition effect when used in the same invasion inhibition assays. Although the influence of the α-Pf332DBL/nDBL-antibodies was slightly lower, these antibodies gave a similar pattern compared to the α-AMA-1/MSP-1 antibodies (Fig. 6), indicating a role of Pf332 during the reinvasion process of the merozoites.

DISCUSSION

Successful attachment of the *P. falciparum* merozoite to the RBC surface is the first important step in the process of invasion and intracellular proliferation. Numerous *in vitro* studies have concluded that the cascade of the rapid invasion process, taking less than 20 seconds [26], is complex and involves a large number of different molecules. Proteins such as the MSPs, AMA-1, EBL- and Rh-family members located in the micronemes, the rhoptries or on the merozoite surface have been shown to play a role in attachment or invasion of the merozoite. However, many aspects of this process remain to be elucidated. The molecule initiating the contact between the merozoite and the RBC is not identified, and the exact location of the invasion process within the human body is still unknown. Furthermore, it is at present unclear as to which molecular events underlie the loss of infectivity, which is observed in merozoites isolated from *in vitro* grown *P. falciparum* parasites.

To shed additional light on the complex process of invasion we have used the genome sequence of *P. falciparum* to identify proteins

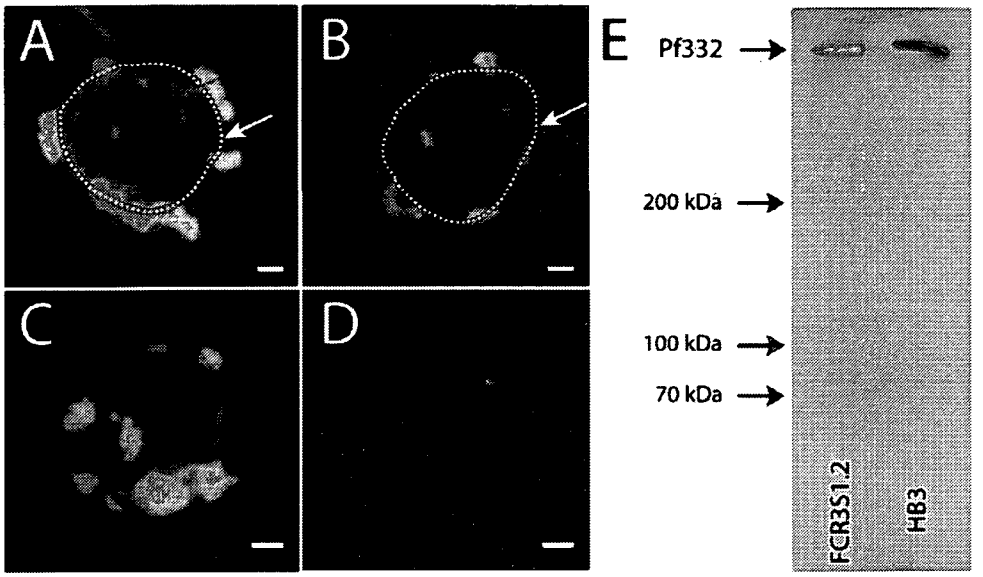

Figure 4. The Pf332 DBL-domain is iRBC surface associated. Immunofluorescence with antibodies against the DBL-domain visualizes the surface association of the Pf332 DBL-domain as shown for HB3 iRBC (**A+C**) and FCR3S1.2 iRBC (**B+D**). **A+B**: Parasites are unstained; the RBC membrane is indicated with a white line/arrow, the intracellular parasite with a grey line/arrow. **C+D**: Parasites are stained orange with Ethidium-bromide. Scale bars = 1 μm. E: Western blot with the same α-Pf332 DBL-domain antibody as used for the immunofluorescence assays; the antibody recognizes only the molecule Pf332 and does not cross-react with any other proteins.
doi:10.1371/journal.pone.0000477.g004

potentially involved in invasion and discovered the ORF PF11_0506 that possesses a RBC-binding domain. Detailed analysis of this gene fragment and the encoded protein has led to several discoveries.

We have here revised the gene structure of Pf332. RT-PCR and Northern blot clearly showed that the two predicted ORF PF11_0506 and PF11_0507 are two exons of a single gene. This conclusion was confirmed by Western blot analysis using three different α-Pf332 antibodies to various regions of the polypeptide. Exon II of Pf332 was initially identified from a gDNA expression library containing only the region of repetitive sequence without additional 5′-RACE sequencing to identify the 5′-end of the transcript [15,27]. The existence of the additional upstream exon in the gene of Pf332 has therefore previously been overlooked and exon I (PF11_0506) was as a consequence annotated in the *P. falciparum* genome as a separate gene encoding a hypothetical protein. Our revision of the gene structure of Pf332 has paved the way to dissect the biological function of Pf332, one of the largest proteins found in *P. falciparum* parasites.

The first exon of Pf332 encodes a conserved erythrocyte-binding domain homologous, but with a distinct sequence, to the DBL-domains of the EBL-family. This sequence is, in contrast to other erythrocyte-binding proteins, conserved among different *P. falciparum* strains and clones. Proteins expressed by the *Plasmodium* parasite often show sequence alterations in regions that are crucial for immunity or undergo antigenic variation, in particular surface related molecules, due to the constant pressure from the host immune system. This also includes members of the EBL-family, as for example the EBA-175, that are conserved only in function but show variation within their sequence [28]. However, the extracellular region of Pf332 displays a conserved sequence, which might ensure the parasite's ability to adhere to RBC independent of the genetic background of the host. The capacity to bind uninfected RBC to the schizont surface might act as a virulence factor for the parasite, and greatly increase the invasion efficiency. Due to the conservation of sequence in the DBL-domain this virulence factor might be primarily of importance in non-immune individuals without prior exposure to the parasite, rapid acquisition of antibodies against this invariable domain in semi-immune individuals could contribute substantially to protection against high multiplication rates of the parasite and therewith against severe disease.

A common feature of *P. falciparum* is that this parasite is able to invade any human RBC, although the efficiency generally depends on the carbohydrate moieties of the glycophorin on the RBC surface. It can be hypothesized that the initial contact between schizont and the RBC is the interaction of a conserved receptor-ligand pair, a function that could be fulfilled by the DBL-domain of Pf332 and an unknown receptor on the RBC surface, while the invasion afterwards is dependant on molecules such as MSP-1 and AMA-1. Numerous laboratory and patient isolates are frequently found to form rosettes during late trophozoite and schizont stage. This rosette formation is irrespective of the "classical rosetting" mediated by PfEMP1 taking place earlier in the parasites lifecycle. Merozoites of these parasites invade more efficiently uninfected RBC involved in these rosettes than into unattached RBC (data not shown). The association of the DBL-domain of Pf332 with the iRBC surface correlates with late stage rosetting, indicating that Pf332 might facilitate invasion for released merozoites through providing close proximity of new host cells. Even though schizonts are often located in capillaries, where the speed of blood flow is reduced due to sequestered and agglutinated iRBC, the newly released merozoites would additionally benefit from a reduced distance towards new host cells. Pf332 might in addition support the invasion process of merozoites after rupture of the schizont. Accumulating amounts of Pf332 during schizont stage might loosely attach to the merozoites surface assisting the parasite to more easily come in contact with and to invade a new host cell after release from the schizont (Fig. S4).

It has previously been suggested that the EB200 region of Pf332 with its degenerative repeats might function as an immunological

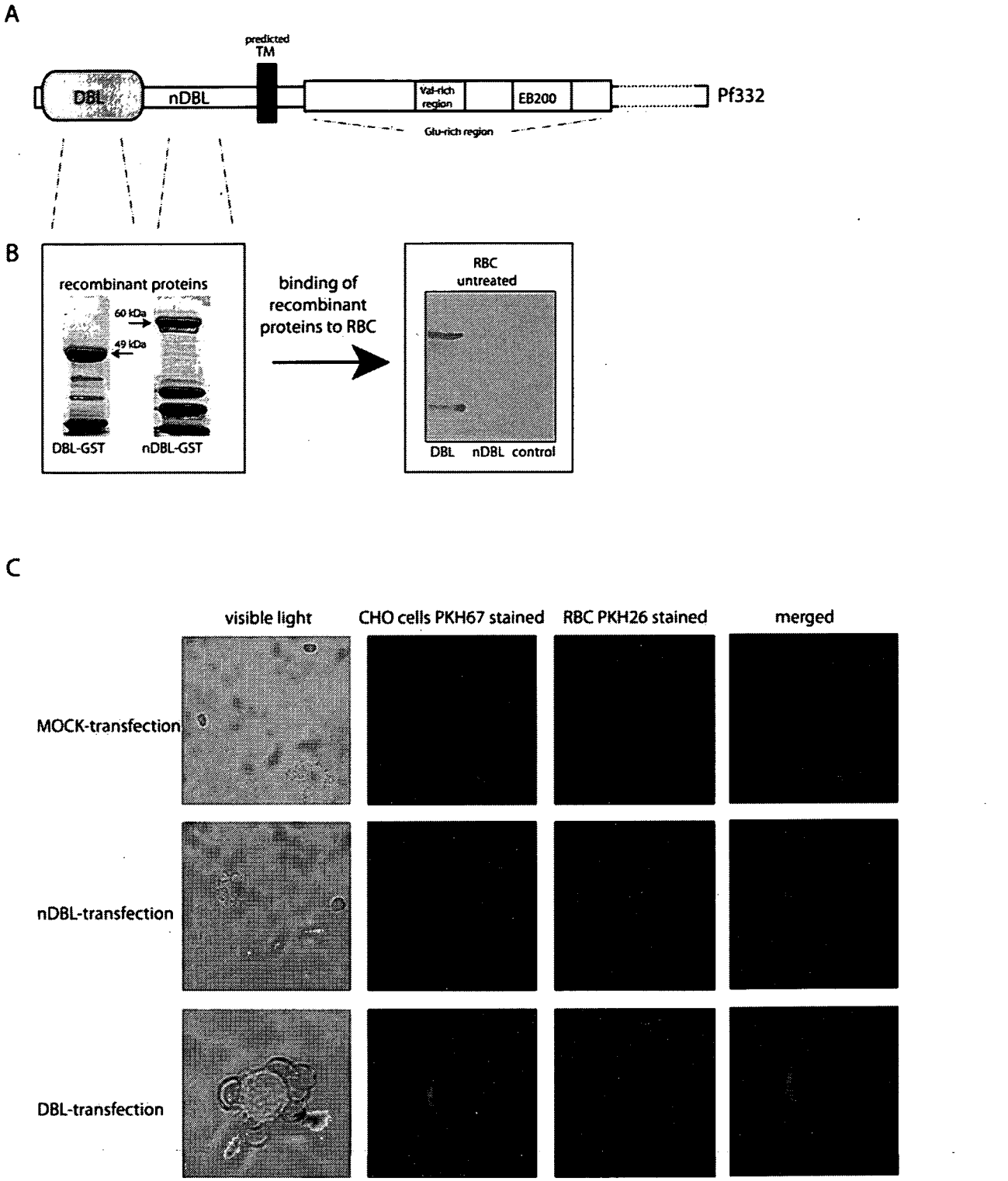

Figure 5. The DBL domain of Pf332 binds to human RBC. A: The protein Pf332 consists of a potentially extracellular region encoded by exon I and is composed of a DBL- and nDBL-domain followed by a predicted transmembrane domain. The region of the molecule originally described as Pf332 is encoded by a second exon and contains a Glutamic-acid rich part, which includes a Valin-rich area as well as the region EB200 build of numerous repeats of a XXXEEXXEEXX motif (X = hydrophobic aa). **B:** The Pf332-DBL- and Pf332nDBL-region were expressed as two individual GST-fusion proteins in E.coli. Binding assays, in which human RBC were incubated with the DBL-, nDBL- and an unrelated control protein were carried out. Binding of the proteins was visualized by subjecting the RBC to immunoblotting, where the bound protein was detected with an α-GST antibody. The DBL- but not the nDBL-domain or the unrelated control protein was able to bind to human RBC. **C:** Transient transfected CHO cells expressing either the DBL- or nDBL-domain on their surface were tested for their ability to bind to human RBC. CHO cells were stained red with PHK26 and incubated with RBC stained green with PKH67. CHO-cells expressing the DBL-domain avidly bound RBC, lower panel, while CHO cells expressing the nDBL-region or MOCK-transfected cells did not show any binding towards RBC (middle and upper panel).
doi:10.1371/journal.pone.0000477.g005

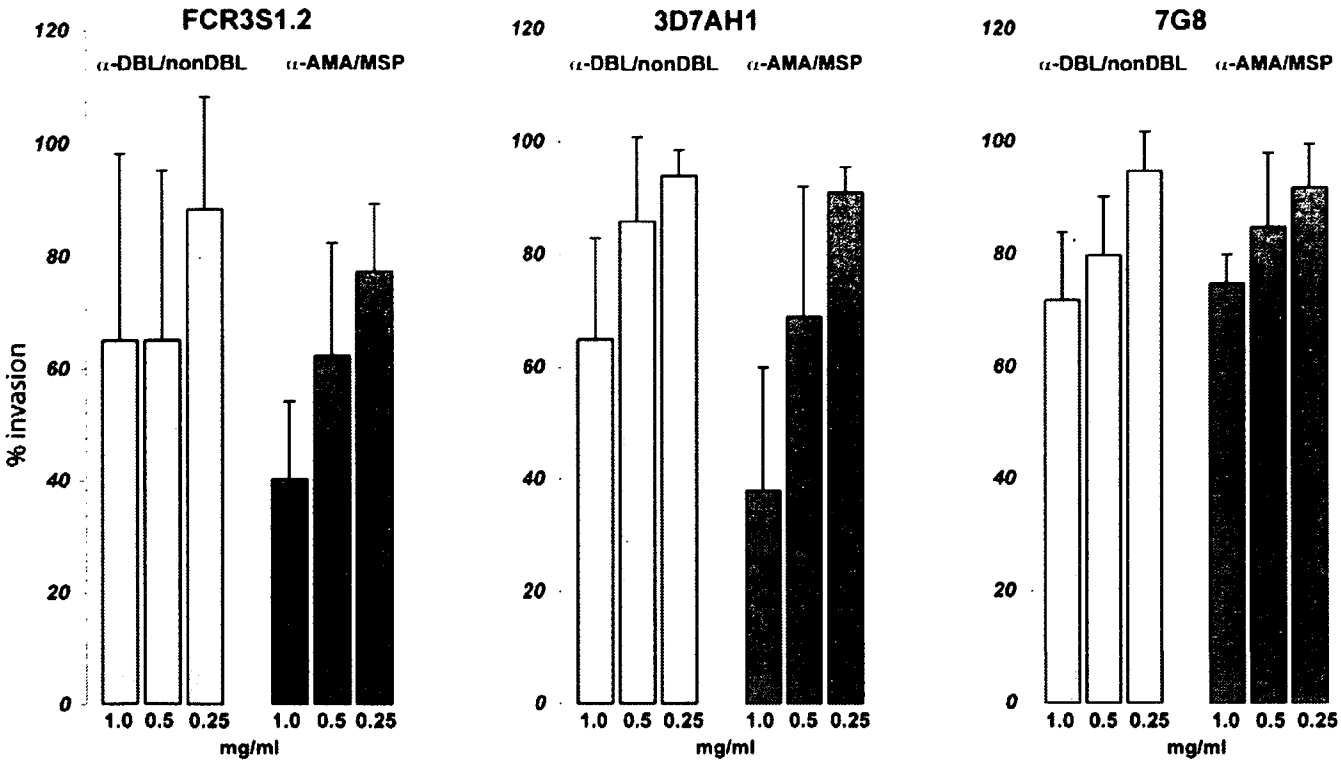

Figure 6. Antibodies directed against the DBL-domain of Pf332 inhibit parasite invasion. RBC infected with the parasite clones/strains FCR3S1.2, 3D7AH1 and 7G8 were cultivated in the presence of α-Pf332-DBL/nDBL-antibodies for 24 h allowing reinvasion of the parasites into new RBC. The parasitemia was analysed by flow-cytometry and compared to a control cultivated in the presence of a serum raised against a non-related protein. Parasites displayed a decreased invasion rate in the presence of α-Pf332-DBL/nDBL-antibodies. The effect of α-Pf332-DBL/nDBL-antibodies (light bars) is slightly lower as compared to inhibition caused by antibodies against a hybrid protein of AMA1 and MSP1 (dark bars). Bars represent the mean of three experiments; error bars indicate the standard deviation.
doi:10.1371/journal.pone.0000477.g006

smokescreen distracting antibodies away from important epitopes of the molecule [29]. In contrast to the DBL-domain, exon II displays sequence polymorphism among different isolates possibly attracting the host immune response and shielding the functional N-terminal region of the molecule. Subsequently, the DBL-domain of Pf332, although exposed in some way to the immune system, is able to retain a conserved sequence mediating the important first step of the process of RBC invasion. Still, the lack of variation of the DBL-domain suggests that it is not overtly exposed to the immunesystem as PfEMP1 or the RIFINs, but concealed prior to exerting it function.

Quantitative differences in expression of Pf332 have been reported from different *P. falciparum* strains in earlier studies [30]. Microarray data presented in the PlasmoDB (http://www.plasmodb.org) show Pf332 to be transcribed in 3D7, Dd2 and HB3 parasites with a higher transcription level in HB3 iRBC than in the other strains. Interestingly, the chromosomal fragment containing the gene of Pf332 is duplicated in the HB3 strain [31]. Here we confirm the transcription and expression of Pf332 by both real-time quantitative PCR and semi-quantitative Western blot analysis. In our quantitative PCR assays, the transcription level of the gene was related to the transcription of *seryl-tRNA synthetase*, a house-keeping gene which is constantly active during the whole erythrocytic cycle of the parasite making it a suitable control for time course studies of gene expression. RNA was collected every 4 hours from 8 h p.i. onwards and transcription of the Pf332 gene was found to start at 16 h p.i. as described before [18,32]. While the transcription pattern was similar in all parasite clones/strains, the transcription level observed in FCR3S1.2 iRBC was more than twice as high as in the other two strains (Fig. 3A), resulting in a significantly higher expression of Pf332 as visualized in Western blot assays (Fig. 3C) indicating a direct relation between Pf332 transcription and expression. Interestingly, among the parasite clones/strains investigated, the FCR3S1.2 clone has the shortest replication cycle (44–46 h instead of 48 h), and in addition an approximately doubled multiplication rate compared to 3D7AH1 iRBC (data not shown) suggesting a potential benefit from increased amounts of Pf332.

To date, the only parasite-derived protein on the iRBC surface that is well characterized is the molecule PfEMP1. However, PfEMP1 is mainly expressed in the earlier trophozoite stage and its foremost function is to mediate adhesion of the iRBC to the vascular endothelium. Pf332 is in contrast expressed at late trophozoite and schizont stage and proposed to be involved in binding of uninfected RBC. Immunofluorescence assays performed in this study and earlier [18] show that Pf332 first accumulates in the parasitophorous vacuole and is thereafter, transported into the erythrocyte cytoplasm where it meets with PfEMP1 and the RIFINs on their way towards the surface of the iRBC. The Pf332 molecule contains four variant antigen-specific translocation signal sequences (PEXEL motifs) [22,23] indicating that this molecule is transported to the RBC surface. While Pf332 and PfEMP1 transiently co-localize in the late trophozoite stage, their distribution pattern within the iRBC again differs during the schizont stage reflecting functional differences of the two molecules. Pf332 is presented later on the surface of the iRBC than PfEMP1 and may participate in the sequestration process of the iRBC in the microvasculature as previously suggested [16];